SecA mediates cotranslational targeting and translocation of an inner membrane protein

Shuai Wang, Chien-I Yang, and Shu-ou Shan

Division of Chemistry and Chemical Engineering, California Institute of Technology, Pasadena, CA

Protein targeting to the bacterial plasma membrane was generally thought to occur via two major pathways: cotranslational targeting by signal recognition particle (SRP) and posttranslational targeting by SecA and SecB. Recently, SecA was found to also bind ribosomes near the nascent polypeptide exit tunnel, but the function of this SecA–ribosome contact remains unclear. In this study, we show that SecA cotranslationally recognizes the nascent chain of an inner membrane protein, RodZ, with high affinity and specificity. In vitro reconstitution and in vivo targeting assays show that SecA is necessary and sufficient to direct the targeting and translocation of RodZ to the bacterial plasma membrane in an obligatorily cotranslational mechanism. Sequence elements upstream and downstream of the RodZ transmembrane domain dictate nascent polypeptide selection by SecA instead of the SRP machinery. These findings identify a new route for the targeting of inner membrane proteins in bacteria and highlight the diversity of targeting pathways that enables an organism to accommodate diverse nascent proteins.

Introduction

Roughly 30% of the genome encodes membrane proteins, which are anchored to cellular membranes via at least one transmembrane domain (TMD) and play diverse physiological roles such as signaling, cell shape maintenance, and cell motility. To attain their proper structure and function, newly synthesized membrane proteins must engage dedicated protein targeting pathways by which they are delivered to the correct membrane destination in the cell (Zhang and Shan, 2014). Mislocalization of membrane proteins not only deprives cells of functional proteins, but it also disrupts cellular protein homeostasis as a result of improper exposure of the hydrophobic TMDs in the cytosol that could lead to aggregation and misfolding. This demands that the targeting processes for membrane proteins act with high efficiency to minimize the exposure of TMDs in the cytosol.

The cotranslational targeting of proteins by signal recognition particle (SRP) is the most well-understood pathway for targeted delivery of integral membrane proteins. SRP recognizes hydrophobic signal sequences or TMDs near the N terminus of nascent proteins as soon as they emerge from the ribosome exit tunnel (Walter et al., 1981; Schaffitzel et al., 2006; Zhang and Shan, 2014). The TMD on the nascent protein is shielded from the cytosol by the M domain of SRP. Through the interaction between SRP and the SRP receptor (SR; termed FtsY in bacteria), the nascent protein is delivered to the SecYEG (or Sec61p) protein translocation machinery on the bacterial inner membrane (or the eukaryotic endoplasmic reticulum; Zhang et al., 2010). SRP-dependent targeting is complete before ∼130 amino acids of the nascent polypeptide C-terminal to the signal sequence or TMD is translated (Siegel and Walter, 1988; Ariosa et al., 2015), and releasing nascent proteins from the ribosome abolishes the targeting of SRP-dependent substrates (Kuruma et al., 2005). In bacteria, SRP is generally thought to mediate the targeted delivery of the majority of inner membrane proteins and several periplasmic secretory proteins that contain highly hydrophobic signal sequences (Luirink and Sinning, 2004; Schibich et al., 2016).

A second major protein-targeting pathway in bacteria uses SecA, with the participation of the chaperone SecB in some cases. The SecB/A pathway targets the majority of secretory and outer membrane proteins via a posttranslational mechanism (Hartl et al., 1990). Substrates entering this pathway contain signal sequences that are less hydrophobic than those that engage SRP/SR (Neumann-Haefelin et al., 2000). These signal sequences are recognized by the preprotein cross-linking domain of SecA, which couples its ATPase cycle to the translocation of substrate proteins across SecYEG (Bauer et al., 2014). The posttranslational chaperone SecB assists in maintaining preproteins in the unfolded translocation-competent state while also delivering these proteins to SecA bound at the inner membrane (Weiss et al., 1988). The posttranslational nature of the SecB/A pathway is supported by the following observations: (A) classic SecB/A-dependent substrate proteins, such as OmpA and

Correspondence to Shu-ou Shan: sshan@caltech.edu

Abbreviations used: BDP, BODIPY-FL; BME, β-mercaptoethanol; FRET, Förster resonance energy transfer; IMV, inner membrane vesicle; IVT, in vitro translation; MBD, MreB-binding domain; NTE, N-terminal element; NTS, N-terminal targeting sequence; RNC, ribosome-nascent chain complex; SR, SRP receptor; SRP, signal recognition particle; SUMO, small ubiquitin-like monitor; TF, trigger factor; TMD, transmembrane domain; U-IMV, urea-washed IMV.

The Rockefeller University Press
J. Cell Biol. Vol. 216 No. 11 3639–3653
https://doi.org/10.1083/jcb.201704036

PhoA, can be efficiently inserted into the membrane without coupling the targeting reaction to protein synthesis (Hartl et al., 1990; Gouridis et al., 2009), indicating that a cotranslational mode of targeting is not mechanistically obligatory for these substrates; (B) the SecA ATPase cycle and its interaction with SecYEG are enhanced by the mature domain of the nascent protein C-terminal to the signal sequence, suggesting that a substantial length of the nascent protein needs to be exposed before they are targeted by the SecB/A pathway (Gouridis et al., 2009); (C) C-terminal fusion to fast-folding proteins such as thioredoxin (TrxA) severely blocks the translocation of SecA-dependent substrate proteins (Huber et al., 2005a), suggesting that targeting and translocation was not finished before the complete synthesis of the nascent polypeptide.

More recently, however, SecA was found to also interact with the ribosome. SecA binds the 70S bacterial ribosome with a dissociation constant (K_d) of 0.9 µM (Huber et al., 2011), in part via an interaction with conserved acidic residues on the L23 protein near the ribosome exit site (Singh et al., 2014). Disruption of this ribosomal contact modestly reduces the translocation efficiency of several secretory proteins (Huber et al., 2011). Nevertheless, a clear understanding for the role and importance of the SecA–ribosome interaction has been lacking. Although SecA has been observed to contact nascent proteins while they are still bound to the ribosome in vitro (Karamyshev and Johnson, 2005; Huber et al., 2016) and in vivo (Randall, 1983), a cotranslational requirement has not been demonstrated for the SecA–preprotein contact nor for the targeting of these secreted proteins, raising questions as to the necessity of recruiting SecA cotranslationally.

Up till now, SRP is the only known factor in bacteria that can cotranslationally target inner membrane proteins. Nevertheless, model SRP substrates are still targeted to the bacterial inner membrane, albeit more slowly, under SRP-depleted conditions (Wickström et al., 2011; Zhang et al., 2012), suggesting the presence of alternative targeting pathways for inner membrane proteins. In addition, SecA is required for the insertion of multiple inner membrane proteins that contain large periplasmic domains (Wolfe et al., 1985; Gebert et al., 1988; Sääf et al., 1995; Traxler and Murphy, 1996), which implicates that SecA plays a role at some stage of the biogenesis of these membrane proteins. Moreover, some inner membrane proteins in *Escherichia coli* depend on SecA rather than SRP for insertion (Ulbrandt et al., 1997; Kihara and Ito, 1998; Rawat et al., 2015). An inner membrane protein, AcrB, showed more severe defects in membrane insertion under SecA-depleted, than SRP-depleted, conditions (Qi and Bernstein, 1999). Recently, Rawat et al. (2015) explored the insertion requirements of two single-span membrane proteins, RodZ and CadC, and suggested the possibility that RodZ is inserted cotranslationally by SecA (Lindner and White, 2014). A common feature of both proteins is a TMD >100 residues downstream of the N terminus and a strict dependence on SecA, but not SRP or FtsY, for insertion. In chloroplasts, cpSecA has been speculated to be an alternative targeting factor, as the cpSecA-dependent substrate protein PetA is cotranslationally targeted to the thylakoid membrane (Zoschke and Barkan, 2015). These observations compel us to explore the possible role of SecA in mediating a potential cotranslational targeting pathway for inner membrane proteins.

Using a combination of quantitative binding measurements, in vitro reconstitutions, and in vivo targeting assays, we demonstrate in this study that SecA cotranslationally recognizes and targets the inner membrane protein RodZ. The extended N-terminal element (NTE) preceding the internal TMD of RodZ and periplasmic sequences immediately after the TMD enable the selection of RodZ by SecA, rather than the SRP machinery, for membrane targeting. This study uncovers a new role of SecA and provides evidence for an SRP-independent cotranslational targeting pathway for a subset of inner membrane proteins in bacteria.

Results

SecA cotranslationally interacts with the RodZ nascent chain

As a candidate substrate that could cotranslationally interact with and be targeted by SecA, we tested RodZ (Rawat et al., 2015). RodZ is a single-pass type II membrane protein comprised of an N-terminal cytoplasmic domain (residues 1–111), a TMD (residues 112–132) anchored on the bacterial plasma membrane, and a C-terminal periplasmic domain (residues 133–337). The in vivo biogenesis of RodZ was shown to be dependent on SecA and SecYEG but had no dependence on the bacterial SRP protein Ffh, the SR FtsY, or the posttranslational chaperone SecB (Ulbrandt et al., 1997; Rawat et al., 2015). As discussed by Rawat et al. (2015), a cotranslational mechanism of targeting would be beneficial for minimizing the cytosolic exposure of the RodZ-TMD and the premature folding of the RodZ periplasmic domain in the cytosol; we therefore hypothesized that SecA could be recruited to ribosome-nascent chain complexes (RNCs) bearing newly synthesized RodZ.

To detect the interaction between RNC_{RodZ} and SecA, we used Förster resonance energy transfer (FRET). As the FRET donor, we used amber suppression technology (Saraogi et al., 2011) to incorporate a fluorescent amino acid, 7-hydroxycoumaryl ethylglycine (Cm), at residue 111 upstream of the RodZ TMD (Fig. 1 A and Table S1). As the FRET accepter, we labeled SecA at residue 12 with BODIPY-FL (BDP). The mutations and fluorescence labeling did not perturb the activity of SecA in mediating posttranslational protein translocation (Fig. S1 A) nor the interaction of RNC with targeting factors (Saraogi et al., 2011). For initial binding measurements, we purified RNC_{RodZ} displaying the N-terminal 180 amino acids of RodZ; the RodZ nascent chain is followed by a 34-residue SecM stalling sequence (Nakatogawa and Ito, 2002), which occupies most of the ribosome exit tunnel (Zhang et al., 2015). When purified RNC_{RodZ} was incubated with $SecA^{BDP}$, we observed a 44% reduction in Cm fluorescence and a corresponding increase in BDP fluorescence, indicating FRET (Fig. 1 B, red). As expected from the competition between labeled and unlabeled SecA, addition of a 10-fold excess of unlabeled SecA removed the FRET signal (Fig. 1 B, blue). This result also ruled out the environmental sensitivity of Cm as a contributor to the FRET signal and indicated a reversible binding equilibrium between RNC_{RodZ} and SecA.

Equilibrium titrations based on the FRET assay showed that SecA binds RNC_{RodZ} tightly, with a K_d value of ∼1 nM (Fig. 1 C); this affinity is ∼900-fold higher than that of SecA for empty ribosomes (Huber et al., 2011), suggesting additional interactions of SecA with the RodZ nascent chain. As other ribosome-associated protein biogenesis factors such as SRP and trigger factor (TF) could compete for binding to the ribosome and RodZ nascent chain under physiological conditions

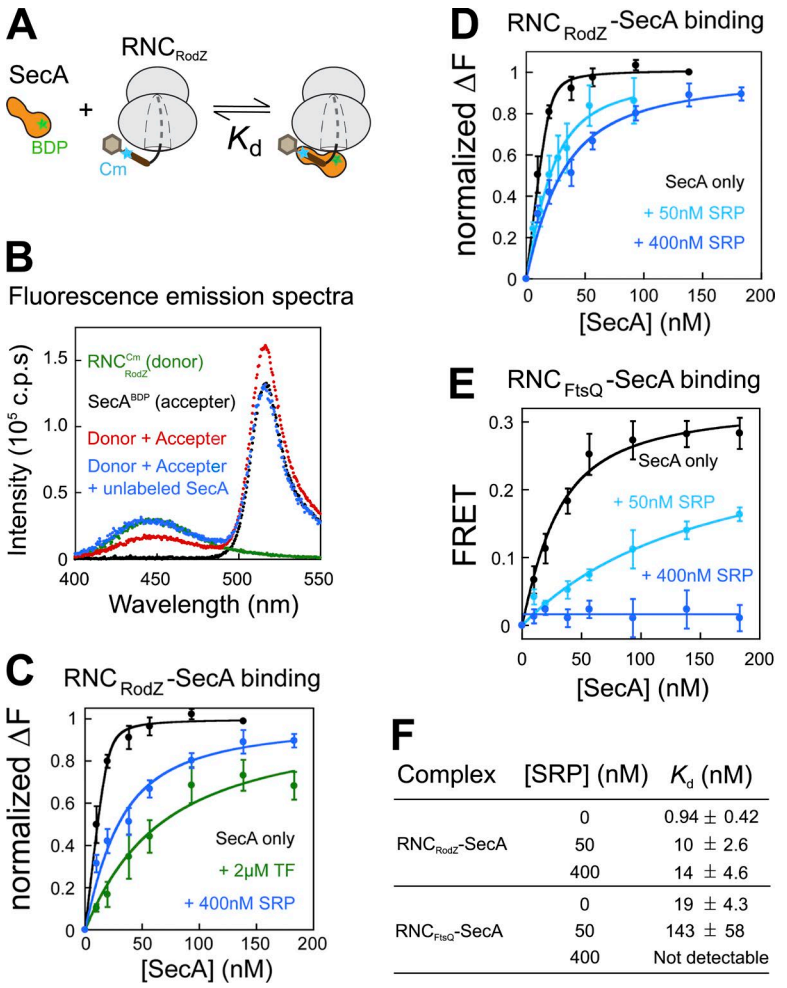

F

Complex	[SRP] (nM)	K_d (nM)
RNC_{RodZ}-SecA	0	0.94 ± 0.42
	50	10 ± 2.6
	400	14 ± 4.6
RNC_{FtsQ}-SecA	0	19 ± 4.3
	50	143 ± 58
	400	Not detectable

Figure 1. **Fluorescence measurements of SecA–RNC interactions.** (A) Scheme of the FRET assay to detect the interaction of SecA with the RodZ nascent chain on the ribosome. (B) Fluorescence emission spectra for indicated samples. Where indicated, reactions contained 20 nM RNC^{Cm}_{RodZ}, 40 nM $SecA^{BDP}$, and 400 nM unlabeled SecA. (C) Representative equilibrium titrations to measure the K_d values of the SecA–RNC_{RodZ} complex. Reactions contained 20 nM RNC^{Cm}_{RodZ} without (black) or with SRP (blue) or TF (green) present. The titration curves before normalization are shown in Fig. S1 B. Lines are fits of the data to Eq. 3. (D and E) Representative equilibrium titrations to measure the K_d values of the SecA–RNC_{RodZ} (D) and SecA–RNC_{FtsQ} (E) complexes at increasing concentrations of SRP. Lines are fits of the data to Eq. 3. (F) Summary of the K_d values of SecA–RNC complexes obtained from the data in C–E and their replicates. Values represent mean ± SD; n = 3.

(Ariosa et al., 2015; Gamerdinger et al., 2015), we further tested whether the SecA–RNC_{RodZ} interaction survives the presence of these factors. Equilibrium titrations in the presence of near-physiological concentrations of SRP (400 nM) or TF (2 µM) showed that the SecA–RNC_{RodZ} interaction was weakened by these factors but remained strong, with K_d values of ∼19 nM and ∼55 nM, respectively (Figs. 1 C and S1 B). In addition, raising the SRP concentration beyond 50 nM did not significantly weaken the binding between SecA and RNC_{RodZ} (Fig. 1, D and F; and Fig. S1 C). As a negative control, we used RNC_{FtsQ}, a well-characterized SRP substrate (Estrozi et al., 2011). Although the interaction of SecA with RNC_{FtsQ} could be detected, this interaction was ∼20-fold weaker than that with RNC_{RodZ} and did not withstand the competition from physiological concentration of SRP (Fig. 1, E and F). These data strongly suggest that the nascent chain of RodZ can efficiently and specifically recruit SecA during translation.

We next asked whether the ribosome contributes to the recruitment of SecA onto nascent RodZ. To this end, we disassembled the ribosomes in purified RNCs by RNase A and EDTA treatment (Fig. S1 D). As an independent and more specific means to perturb the SecA–ribosome interaction, we mutated an acidic patch (F51A/E52A/E54A/E56A/E89A) on the ribosomal protein L23 that contacts the N terminus of SecA (Fig. 2 A; Huber et al., 2011; Singh et al., 2014). Both perturbations significantly weakened the interaction of SecA with the RodZ nascent chain. The L23 mutations weakened the binding affinity of SecA for RNC_{RodZ} >20-fold (Fig. 2, B and E, red). The binding defect was larger, ∼60-fold, with EDTA- and RNase A–treated RNC_{RodZ} (Fig. 2, B and E, blue). As a negative control, we tested RNC bearing the nascent chain of PhoA, a posttranslational SecA substrate (Gouridis et al., 2009). Although an interaction between SecA and RNC_{PhoA} could be detected, neither the L23 mutations nor the EDTA–RNase A treatment affected this interaction (Fig. 2, C and E), indicating that SecA binds the PhoA nascent chain independently of the ribosome. As a positive control, the interaction of SRP with its substrate, RNC_{FtsQ}, was also disrupted by the RNase A and EDTA treatment (Fig. 2, D and E, blue). However, SRP-RNC_{FtsQ} binding was unaffected by the L23 mutations (Fig. 2, D and E, red), indicating that this acidic patch on L23 provides a specific docking site for SecA. These results show that efficient recruitment of SecA to the RodZ nascent chain requires specific contacts of SecA with the ribosomal protein L23.

SecA recognizes multiple sequence elements on the RodZ nascent chain

To probe the sequence elements on the RodZ nascent chain required for SecA recognition, we first tested the role of the RodZ TMD (Fig. 3 A). Introduction of two arginines weakened the SecA–RodZ interaction ∼26-fold, raising the K_d value to ∼26 nM (Fig. 3 B, TMD mut). Introduction of six basic residues into RodZ-TMD abolished detectable interaction of SecA with the

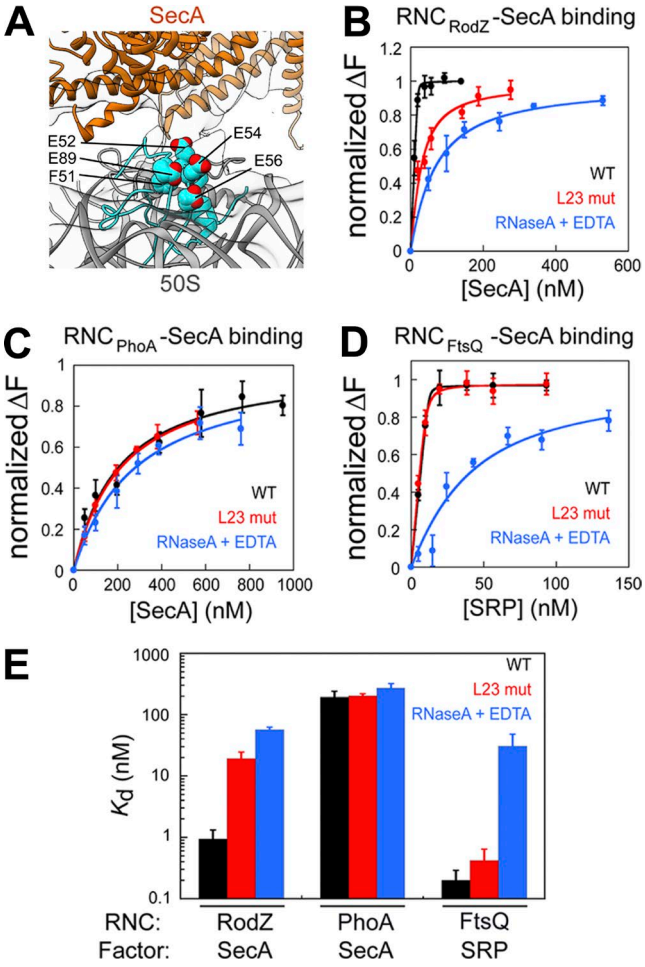

Figure 2. **Contribution of the ribosome to RNC–SecA affinity.** (A) Structure of SecA bound to the 70S ribosome (EMD-2565). The crystal structures of SecA (PDB 1m6n; orange) and ribosome (PDB 2aw4; gray) were docked into the EM density. Residues on L23 (cyan) that contact SecA are in *space-fill*. (B–D) Equilibrium titrations to measure the affinity of SecA for WT and modified RNC_{RodZ} (B) and RNC_{PhoA} (C) as well as the affinity of SRP for RNC_{FtsQ} (D). Lines are fits of the data to Eq. 3. (E) Summary of the K_d values derived from the data in B–D. Values represent mean ± SD; $n = 3$.

nascent chain (Fig. 3 B, 3K3R mut). These results suggest that the hydrophobic TMD on RodZ provides an important recognition element for SecA.

If SecA recognizes the TMD on RNC_{RodZ}, then the SecA–RNC_{RodZ} interaction would be sensitive to the length of the nascent polypeptide, as complete exposure of the TMD on the ribosome would require at least 133 amino acids of the RodZ nascent chain to be displayed on the stalled RNC. We therefore systematically varied the length of the RodZ nascent chain (length does not include the SecM arrest sequence). As expected, SecA binding was barely detectable when the RodZ nascent chain was 120 amino acids, at which length only a portion of the TMD was available (Figs. 3 C and S1 E, inset). Significantly stronger SecA binding was observed at longer nascent chain lengths, with the tightest binding observed when the RodZ nascent chain was 160 amino acids (Fig. 3 C). Collectively, these data strongly suggest that SecA recognizes the TMD of the RodZ nascent chain.

The RodZ TMD is preceded by an extended NTE comprised of a helical MreB-binding domain (MBD; residues 1–103) followed by a consecutive sequence of six basic residues (KRRKKR; residues 104–109). Deletion of the MBD did not perturb high-affinity binding between SecA and RNC_{RodZ}, whereas deletion of the basic residues preceding the TMD weakened binding >10-fold (Fig. 3, D–F). These results are consistent with previous findings that positively charged residues N-terminal to the signal sequence enhance preprotein binding and translocation by SecA (Akita et al., 1990; Hikita and Mizushima, 1992).

The enhancement in the RNC binding affinity of SecA when the RodZ nascent chain was lengthened from 140 to 160 amino acids suggests the possibility of additional interactions of SecA with the periplasmic sequence of RodZ after the TMD. To test this hypothesis, we replaced the sequences in the N-terminal periplasmic region of $RNC_{RodZ160}$ (residues 134–160) with the corresponding sequence from FtsQ (Fig. 3 D, Peri swap). This mutation weakened the affinity of SecA for $RNC_{RodZ160}$ >40-fold (Fig. 3, E and F), indicating that the periplasmic sequence of RodZ after its TMD also contributes significantly to high-affinity SecA recruitment. Intriguingly, this periplasmic region of RodZ does not belong to the "hydrophobic patch" that binds SecA as described by previous studies (Gouridis et al., 2009; Chatzi et al., 2017), but is instead unusually enriched in acidic residues (net charge −4) compared with the corresponding region of FtsQ (net charge 0; Table S1). To test whether these acidic residues contribute to SecA recruitment, we further incorporated the acidic residues in the periplasmic region of SecA into the corresponding positions in the FtsQ periplasmic sequence (R54E/K59E/R66E/H67D/R70D; Fig. 3 D, Peri swap acidic). The incorporation of these additional acidic residues indeed restored high-affinity SecA binding (Fig. 3, E and F, peri swap vs. peri swap acidic), indicating the importance of these acidic residues in SecA recognition.

Finally, to distinguish whether the periplasmic sequence of RodZ exerts its effect directly by interacting with SecA or indirectly by altering the conformation of the remainder of the RodZ nascent chain, we fused this sequence (RodZ residues 134–160) or the corresponding periplasmic sequence from FtsQ (residues 50–74) to the well-folded small ubiquitin-like modifier (SUMO) protein. We tested whether the resulting fusion proteins acted as competitive inhibitors of the interaction between SecA and RNC_{RodZ}. If the periplasmic sequence of RodZ directly bound SecA, SUMO-RodZ(peri) should be able to compete with RNC_{RodZ} for SecA binding and thus restore the fluorescence signal of donor-labeled RNC caused by loss of FRET between RNC^{Cm} and $SecA^{BDP}$ (Fig. 3 G). Dose-dependent saturable restoration of the fluorescence of RNC^{Cm} was indeed observed with SUMO-RodZ(peri) (Fig. 3 H). In contrast, SUMO by itself did not compete with RNC_{RodZ}, and SUMO-FtsQ(peri) provided significantly less effective competition than SUMO-RodZ(peri) (Fig. 3 H). Quantitative analysis of this competition reaction yielded an estimated K_i value of 1.2 µM for the interaction between SecA and SUMO-RodZ(peri).

Collectively, the results in this section show that the strong interaction of RNC_{RodZ} with SecA are contributed by three sequence elements on the RodZ nascent chain: (A) the consecutive positively charged residues upstream of the RodZ TMD, (B) the hydrophobic TMD of RodZ, and (C) the negatively charged residues in the periplasmic region of RodZ after its TMD. It is likely that each of these elements contributes a modest affinity, but together they enable high-avidity SecA recognition by providing multiple simultaneous interactions.

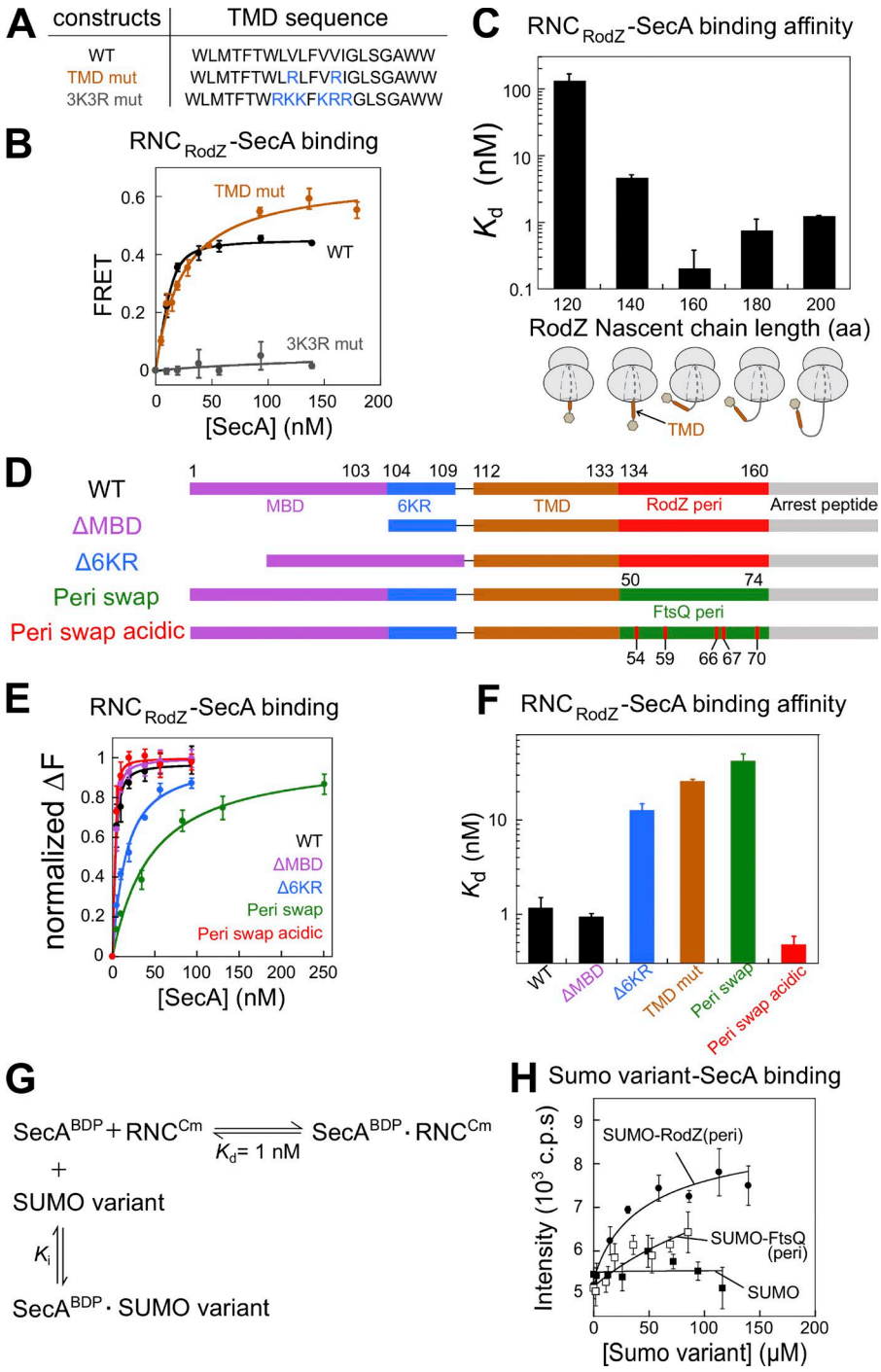

Figure 3. **Defining the sequence elements of RodZ for SecA recognition.** (A) Sequences of TMD in WT RodZ and RodZ TMD mutants. Letters in blue indicate positively charged residues. (B) Equilibrium titrations to measure the affinity of SecA for RNC_{RodZ} bearing WT and mutant TMD sequences. The data were fit to Eq. 2 and gave K_d values of 0.94 ± 0.42 and 25.9 ± 1.1 nM for WT and TMD mut, respectively. (C) Summary of the K_d values at indicated lengths of the RodZ nascent chain (sequences in Table S1) obtained from the data in Fig. S1 E as well as their replicates. Schemes for RNC_{RodZ} at each chain length are shown below the graph, with ribosome in gray, RodZ TMD in brown, and sequences upstream of TMD depicted as hexagons. (D) Scheme of sequence elements in WT and mutant RodZ nascent chain used for the RNC–SecA binding measurements in E and F. MBD (purple) denotes the maltose-binding protein (residues 1–103), 6KR (blue) denotes the ^{104}KKRKRR^{109} sequence, the RodZ TMD is in brown, and RodZ peri (red) and FtsQ peri (green) denote the early periplasmic regions of RodZ (residues 134–160) and FtsQ (residues 50–74), respectively. Mutations to acidic residues at corresponding positions of the RodZ periplasmic sequence are indicated in the Peri swap acidic construct. All the mutant constructs are derived from RodZ160 in Fig. 3 C. See Table S1 for detailed sequences. (E) Equilibrium titrations to measure the binding of SecA to RNCs bearing the WT and mutant RodZ nascent chain depicted in D. (F) Summary of the K_d values for RNCs bearing WT and mutant RodZ nascent chain obtained from the data in B and E. (G) Scheme for the competition assay to measure the binding of SUMO fusion proteins to SecA. BDP-labeled SecA was allowed to form a complex with RNC^{Cm}. This binding equilibrium is perturbed if the inhibitor binds $SecA^{BDP}$ and traps it into a SecA · SUMO variant complex, generating free RNC^{Cm} and resulting in loss of FRET (i.e., increase of Cm fluorescence). (H) Competition reactions to measure the binding of SUMO and SUMO variants to SecA. SUMO, SMT3 residues 1–101; SUMO-RodZ(peri), SMT3 fused to the N terminus of RodZ periplasmic region (residues 134–160); SUMO-FtsQ(peri), SMT3 fused to the N terminus of FtsQ periplasmic region (residues 50–74). The data with SUMO-RodZ(peri) were fit to Eq. 8 and gave a K_i value of 1.2 ± 0.7 μM. In contrast, SUMO and SUMO-FtsQ(peri) did not give robust competition. Values represent mean ± SD; n = 2–3. c.p.s., counts per second.

RodZ is cotranslationally targeted and translocated in vivo independently of SRP

The cotranslational recruitment of SecA to nascent RodZ in vitro raised the possibility of SecA-mediated targeting and translocation of RodZ. Previous work showed that the in vivo insertion of RodZ is strictly SecA dependent (Rawat et al., 2015). To further test whether the targeting and translocation of RodZ occurred cotranslationally, we adapted a previously developed in vivo assay based on fusion of the N-terminal targeting sequence (NTS; Fig. 4 A and Table S1) of the protein of interest to TrxA (Schierle et al., 2003; Huber et al., 2005b). TrxA folds rapidly and tightly in the cytosol, which would block its translocation across the membrane if targeting and translocation of the fusion protein occurred after the C-terminal TrxA is fully synthesized. Only if the NTS enables a cotranslational mode of targeting and translocation would TrxA be successfully translocated across the inner membrane (Fig. 4 A). A Myc tag at the C terminus of NTS-TrxA constructs allowed us to monitor the localization of the fusion protein in cell fractionation experiments. In addition, secretory proteins contain signal sequences that are cleaved by the signal peptidase upon successful translocation across the inner membrane (Fig. 4 A), providing an independent readout for their secretion into periplasm. For proteins that contain a TMD anchored in the bacterial inner membrane, successful translocation of TrxA across the inner membrane exposes the Myc tag to the periplasm, where it is susceptible to proteinase

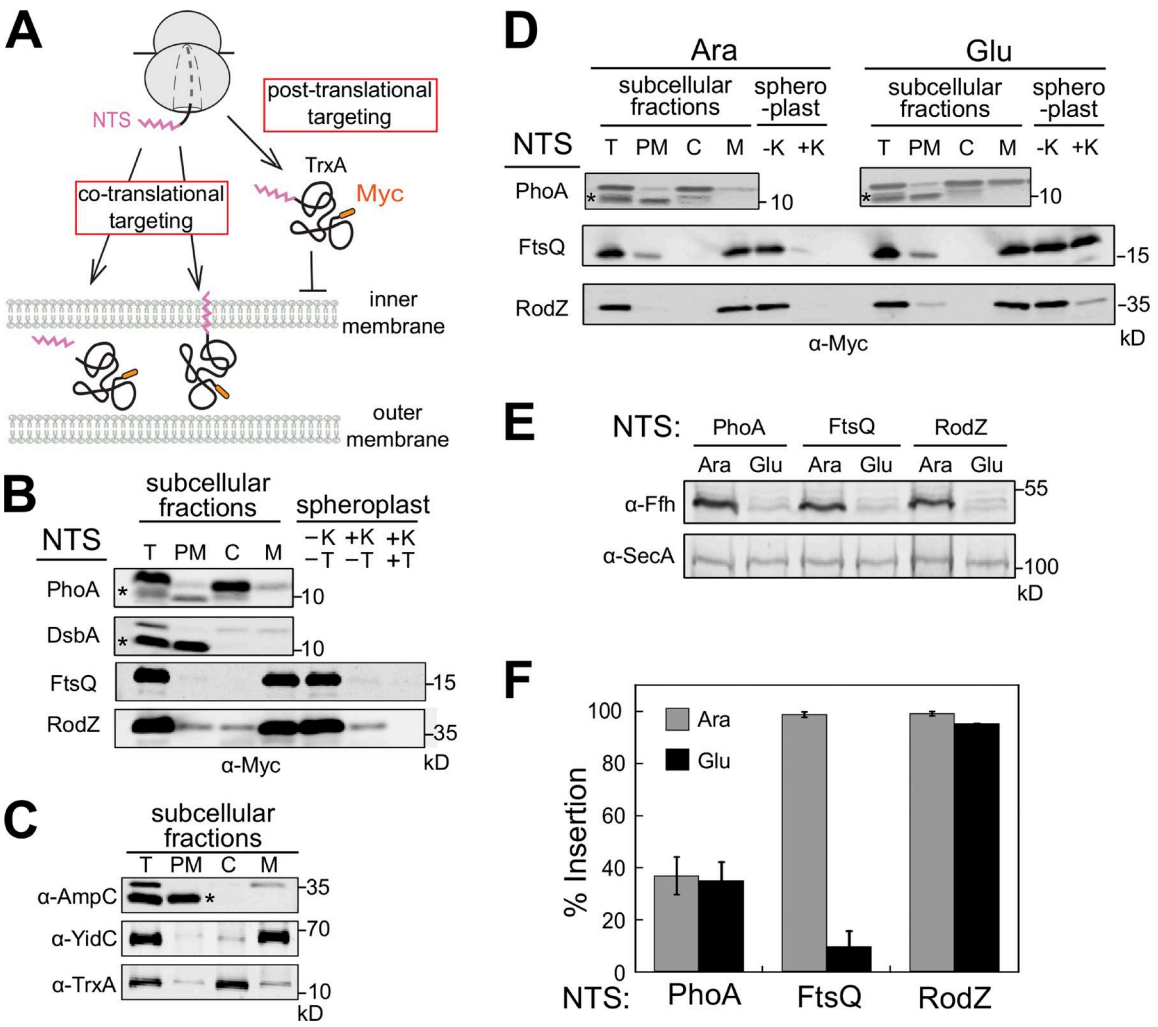

Figure 4. **RodZ is cotranslationally targeted and translocated in vivo.** (A) Scheme of the in vivo assay to distinguish between co- and posttranslational modes of targeting and translocation based on NTS-TrxA fusions. All NTS sequences are provided in Table S1. (B, left) Subcellular localization of NTS-TrxA fusion proteins. C, cytosol; M, membrane; PM, periplasm; T, total. (B, right) Assay for translocation of the C terminus of the NTS-TrxA fusion proteins into periplasm based on protection against proteinase K. K, proteinase K; T, Triton X-100. (C) Controls for cell fractionation. Mature AmpC is secreted into the periplasm (asterisk). YidC is an inner membrane protein. TrxA is a cytoplasmic protein. (D) Effects of Ffh depletion on the targeting and translocation of NTS-TrxA fusions. In vivo targeting and insertion were measured and analyzed as in B. Ffh expression is under control of the arabinose promoter. (E) Ffh is depleted in WAM121 cells grown in glucose without significantly affecting SecA abundance. (F) Translocation efficiency of NTS-TrxA constructs derived from the data in D and their replicates. Asterisks in B–D denote mature translocated secretory proteins whose signal sequences have been cleaved. Values represent mean ± SD; *n* = 2–3 biological replicates.

K digestion (Fig. 4 A); this provides an independent readout for the proper insertion of the fusion protein at the inner membrane.

When the PhoA signal sequence (residues 1–21; Table S1) was used as the NTS, only a small fraction of the fusion protein was successfully translocated into the periplasm (Fig. 4, B and C), consistent with previous work showing that PhoA is primarily posttranslationally targeted by SecA (Schierle et al., 2003; Gouridis et al., 2009). As previously reported (Schierle et al., 2003), the more hydrophobic signal sequence from DsbA (residues 1–19; Table S1) enabled efficient translocation of TrxA into the periplasm (Fig. 4 B). The N-terminal sequence containing the TMD of FtsQ (residues 1–33; Table S1), a substrate of the cotranslational SRP pathway, directed efficient targeting of the fusion protein to the inner membrane (Fig. 4 B). The C-terminal Myc tag in FtsQ(1–33)-TrxA was susceptible to proteinase K digestion in spheroplasts, indicating that its C terminus was successfully translocated across the bacterial inner membrane (Fig. 4 B). These data validated the robustness of the TrxA-based assay to distinguish co- versus posttranslational modes of targeting and insertion in vivo. Importantly, when RodZ residues 1–150 encompassing its TMD was fused to TrxA (Table S1), the fusion protein was efficiently targeted to and translocated across the bacterial inner membrane analogously to FtsQ (Fig. 4 B), indicating that the RodZ-TrxA fusion protein was cotranslationally targeted and inserted in vivo.

To further test the dependence of the targeting reaction on the SRP protein Ffh, we used the WAM121 strain in which Ffh expression is under control of the *ara* promoter (de Gier et al., 1996). In contrast to FtsQ, which depends on Ffh for proper insertion into the membrane, RodZ was not sensitive to Ffh depletion (Fig. 4, D and F), consistent with previous studies showing that RodZ requires SecA, but not SRP nor the SR FtsY, for membrane insertion (Ulbrandt et al., 1997; Rawat et al., 2015). Thus, the N-terminal sequence of RodZ is sufficient to direct the cotranslational targeting of the remainder of the protein via an SRP-independent pathway.

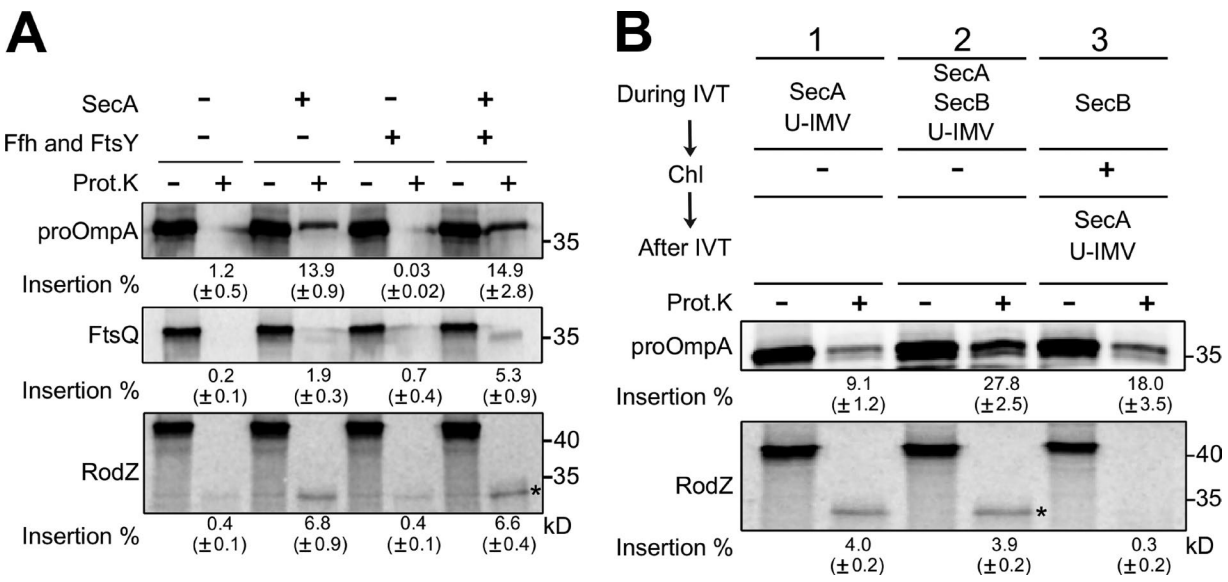

Figure 5. **Reconstitution of RodZ targeting and translocation in vitro.** (A) Effect of SecA and SRP/FtsY on the translocation of indicated substrates into U-IMVs during PURE IVT. Reactions contained 400 nM Ffh, 1 µM FtsY, and 0.94 µM SecA where indicated. 4.5S RNA was included in the tRNA mix (Kuruma et al., 2005). (B) Targeting and translocation of RodZ is strictly cotranslational, whereas that of proOmpA is not. Reactions contained 0.94 µM SecA and 2.5 µM SecB where indicated. Chl, chloramphenicol. Values under each lane are quantifications of percent translocation from these data and their replicates (Fig. S3) and represent mean ± SD; n = 2–3. Asterisks denote the protected fragment after proteinase K digestion.

Although SecA dependence was observed for the targeting and translocation of all the NTS-TrxA fusion proteins tested in the in vivo assay (Fig. S2 A), these data likely reflect a requirement for SecA during the translocation of the TrxA moiety and cannot be used to conclusively infer the involvement of SecA in their targeting (Schierle et al., 2003). In addition, in vivo experiments could only demonstrate the requirement, but not sufficiency, for specific factors. These limitations were addressed by in vitro reconstitution experiments described in the next section.

SecA provides the minimal factor sufficient to drive the cotranslational targeting and insertion of RodZ in vitro

We sought to reconstitute the targeting and insertion of nascent RodZ using the PURE in vitro translation (IVT) system (Shimizu et al., 2001) coupled with urea-washed inner membrane vesicles (IMVs; U-IMVs; Kuruma et al., 2005); successful translocation of substrate proteins across U-IMVs leads to their partial or complete protection from proteinase K digestion. This homologous IVT translocation system contains no endogenous targeting factors, allowing us to probe the contribution of specific factors to the targeting and translocation of protein substrates of interest.

OmpA is a well-studied outer membrane protein that is posttranslationally targeted and translocated by SecA (Hoffschulte et al., 1994; Kuruma et al., 2005). Consistent with these expectations, proOmpA exhibited SecA-dependent but SRP- and FtsY-independent targeting and translocation across U-IMVs in the IVT translocation assay (Fig. 5 A and replicates in Fig. S3 A). However, FtsQ requires SRP and FtsY for targeting to the membrane and SecA for translocation of its periplasmic loop (Scotti et al., 1999; Kuruma et al., 2005). The coupled IVT translocation assay recapitulated the dependences of FtsQ on both factors (Fig. 5 A and replicates in Fig. S3 A). Importantly, RodZ was inserted in the presence of SecA alone in this assay, and the additional presence of SRP/FtsY did not improve its translocation efficiency (Fig. 5 A and Fig. S3). These data are consistent with the in vivo observation that RodZ requires SecA but not SRP and FtsY for its proper biogenesis (Fig. 4; Ulbrandt et al., 1997; Rawat et al., 2015). Moreover, they strongly suggest that SecA provides the minimal factor that can mediate the targeting and insertion of newly synthesized RodZ.

To test the cotranslational requirement for RodZ insertion in this assay, we changed the order of addition of targeting/translocation components. Robust insertion of RodZ was only observed if SecA and U-IMVs were added during IVT (Figs. 5 B and S3 B, reaction 1). In contrast, if SecA and U-IMVs were added after termination of translation by chloramphenicol, no insertion was observed (Figs. 5 B and S3 B, reaction 3). Under this obligatorily posttranslational condition, proOmpA was still efficiently inserted, albeit with lower efficiency than if SecA and U-IMVs were supplied during IVT (Figs. 5 B and S3 B, reactions 2 vs. 3). Finally, although inclusion of the posttranslational chaperone SecB improved the insertion efficiency of proOmpA as previously described (Kuruma et al., 2005), SecB did not affect the targeting and insertion of RodZ (Figs. 5 B and S3 B, reactions 1 vs. 2; Rawat et al., 2015). Collectively, these results support the model that SecA provides the minimal machinery sufficient for the cotranslational targeting and insertion of RodZ.

The extended NTE and early periplasmic region of RodZ dictate its selection by SecA over SRP

The majority of the bacterial inner membrane proteome is generally thought to be targeted by SRP, which recognizes hydrophobic TMDs or signal sequences on the nascent polypeptide. The observation that SecA also cotranslationally recognizes the RodZ-TMD raises the intriguing question of how nascent membrane proteins are selected between these two factors. Comparison of RodZ with well-studied SRP substrates such as FtsQ suggested the 111-residue NTE of RodZ preceding its TMD

as a potential distinguishing feature. Another SecA substrate, EspP, was shown to be excluded from the SRP pathway because of its extended NTE, and deletion of this NTE reroutes EspP to the SRP pathway (Peterson et al., 2003; von Loeffelholz et al., 2013). We therefore hypothesized that, analogous to EspP, the extended NTE of RodZ disfavors its engagement with SRP.

To test this hypothesis, we deleted the NTE of RodZ ($RodZ^{\Delta NTE}$) or fused the RodZ NTE to the N terminus of FtsQ-TMD (RodZNTE-FtsQ; Fig. 6 A and Table S1). We tested the effects of this mutation on multiple activities: (A) the binding affinity of SecA and SRP for RNCs displaying WT and mutant nascent chains (Fig. 6, B and C); (B) the SecA and SRP dependence of preprotein targeting and translocation across U-IMVs in vitro (Fig. 6, D–G); and (C) the SRP dependence of translocation of NTS-TrxA fusion proteins in vivo (Fig. S2, C and D). Deletion of the NTE significantly weakened the binding of SecA to RNC_{RodZ}, and the weakened binding was exacerbated in the presence of competing TF and SRP (RodZ vs. $RodZ^{\Delta NTE}$; Fig. 6 B). $RodZ^{\Delta NTE}$ also exhibited more reduced SecA-dependent targeting and translocation across U-IMVs in vitro than RodZ (Fig. 6 D). These results are consistent with our earlier finding that the basic residues in the RodZ NTE are important for high-affinity SecA recruitment (Fig. 3 C).

However, deletion of the NTE from RodZ enabled strong SRP binding to the RNC even in the presence of competing SecA and TF (RodZ vs. $RodZ^{\Delta NTE}$; Fig. 6 C). In agreement with the binding data, deletion of the NTE converted RodZ into an SRP-dependent substrate in the IVT translocation assay in vitro (Fig. 6 E) and increased the SRP dependence of the translocation of RodZ-TrxA fusion proteins in vivo (RodZ vs. $RodZ^{\Delta NTE}$; Fig. S2, C and D). These data suggest that the NTE of RodZ disfavors SRP binding. As predicted from this hypothesis, fusion of the RodZ NTE to the N terminus of FtsQ TMD destabilized SRP binding to RNC_{FtsQ} in the presence of SecA and TF (FtsQ vs. RodZNTE-FtsQ; Fig. 6 C, black bars). Consistent with these binding data, fusion to the RodZ NTE also abolished the SRP dependence of FtsQ targeting to U-IMVs in vitro (FtsQ vs. RodZNTE-FtsQ; Fig. 6 G) and reduced the SRP dependence of the targeting and insertion of FtsQ-TrxA in vivo (FtsQ vs. RodZNTE-FtsQ; Fig. S2, C and D). Thus, the N-terminal extension of RodZ is necessary and sufficient to prevent the nascent protein from engaging the SRP-targeting machinery.

However, fusion of the RodZ NTE to the N terminus of FtsQ did not confer tight SecA binding (RodZNTE-FtsQ; Fig. 6 B) nor efficient SecA-dependent targeting into U-IMVs (RodZNTE-FtsQ; Fig. 6 F), indicating that the NTE of RodZ is not sufficient to reroute an SRP substrate to a SecA-dependent pathway. Because the periplasmic region of RodZ after its TMD is also important for high-affinity SecA recognition (Fig. 3), we further replaced the sequences in the FtsQ periplasmic domain after its TMD (residues 50–74) with the corresponding sequence from RodZ (RodZ NTE-peri-FtsQ; Fig. 6 A). RNCs bearing the resulting construct bound tightly to SecA (Fig. 6 B) and displayed SecA-dependent targeting and insertion into U-IMVs in vitro (Fig. 6 F). RodZ NTE-peri-FtsQ did not bind strongly to SRP (Fig. 6 C) nor was it targeted and inserted into U-IMVs in an SRP-dependent manner (Fig. 6 G), indicating that it resembles RodZ as a SecA-dependent and SRP-independent substrate. Thus, the extended NTE together with the early periplasmic region of RodZ are sufficient to reroute an SRP-dependent membrane protein into the alternative SecA-mediated cotranslational targeting pathway.

Discussion

Protein targeting to the bacterial cytoplasmic membrane was generally thought to occur via two major pathways (Fig. 7). The majority of periplasmic, secretory, and outer membrane proteins contain weakly hydrophobic signal sequences and are targeted posttranslationally with or without the aid of the chaperone SecB to SecA–SecYEG complexes that translocate preproteins across the inner membrane (Fig. 7, left path). Proteins containing TMDs or highly hydrophobic signal sequences near the N terminus are recognized by SRP as soon as they emerge from the ribosome exit tunnel and are delivered cotranslationally to the SecYEG translocation machinery via interaction between SRP and the SR (Fig. 7, right path). This work demonstrates the existence of an alternative targeting route mediated by SecA for cotranslational targeting to SecYEG sites and integration into the membrane (Fig. 7, middle path). The complete repertoire of substrate proteins using this targeting route remains to be defined. Nevertheless, together with the finding of other substrates that exhibit distinct requirements for alternative translocases (Samuelson et al., 2000; van der Laan et al., 2004), our results add to the diversity of protein-targeting mechanisms in bacteria.

SecA is an essential ATPase in bacteria known to drive the posttranslational translocation of secretory and outer membrane proteins across the SecYEG translocation machinery. The recent findings that SecA also binds ribosomes near the nascent polypeptide exit site (Huber et al., 2011; Singh et al., 2014) suggest additional roles for this protein, but the function of the SecA–ribosome interaction has been unclear. The previous model, in which nascent proteins contact SecA during translation and then engage SecB for membrane delivery after they are released from the ribosome (Huber et al., 2011), regresses to a largely posttranslational mechanism of targeting. The results in this study demonstrate a new possibility: SecA can specifically recognize and mediate the targeting/translocation of some inner membrane proteins in a strictly cotranslational manner. Although the interactions of SecA with nascent periplasmic and outer membrane proteins have been previously characterized and are known to facilitate translocation (Karamyshev and Johnson, 2005; Huber et al., 2011, 2016), the interaction and activity of SecA on the RodZ nascent chain observed in this study is the first example in which the cotranslational mode of SecA action is mechanistically obligatory for the proper biogenesis of the substrate protein. Thus, this work provides a potential mechanism by which the SecA–ribosome interaction plays an essential role in nascent protein biogenesis. Additional mechanistic roles for the SecA–ribosome interaction include providing an early chaperone for nascent polypeptides or facilitating the translocation of large periplasmic loops for proteins still bound to the ribosome; these possibilities remain to be explored.

Nascent RodZ was shown to bind SRP in ribosome profiling experiments (Schibich et al., 2016). This is consistent with our observation in this study that RodZ still binds SRP with a K_d value of 24 nM in the presence of physiological concentrations of TF and SecA (Fig. 6 C). Indeed, SRP altered the FRET value of the RNC–SecA complex, and the weakening effect of SRP on RNC–SecA binding saturated at SRP concentrations above 50 nM (Fig. S1 C). These observations argue against a model in which the binding of SRP and SecA to RNC_{RodZ} is mutually exclusive and instead are more consistent with a model in which these two factors allosterically modulate the affinity and conformation of one another at the ribosome exit site (see

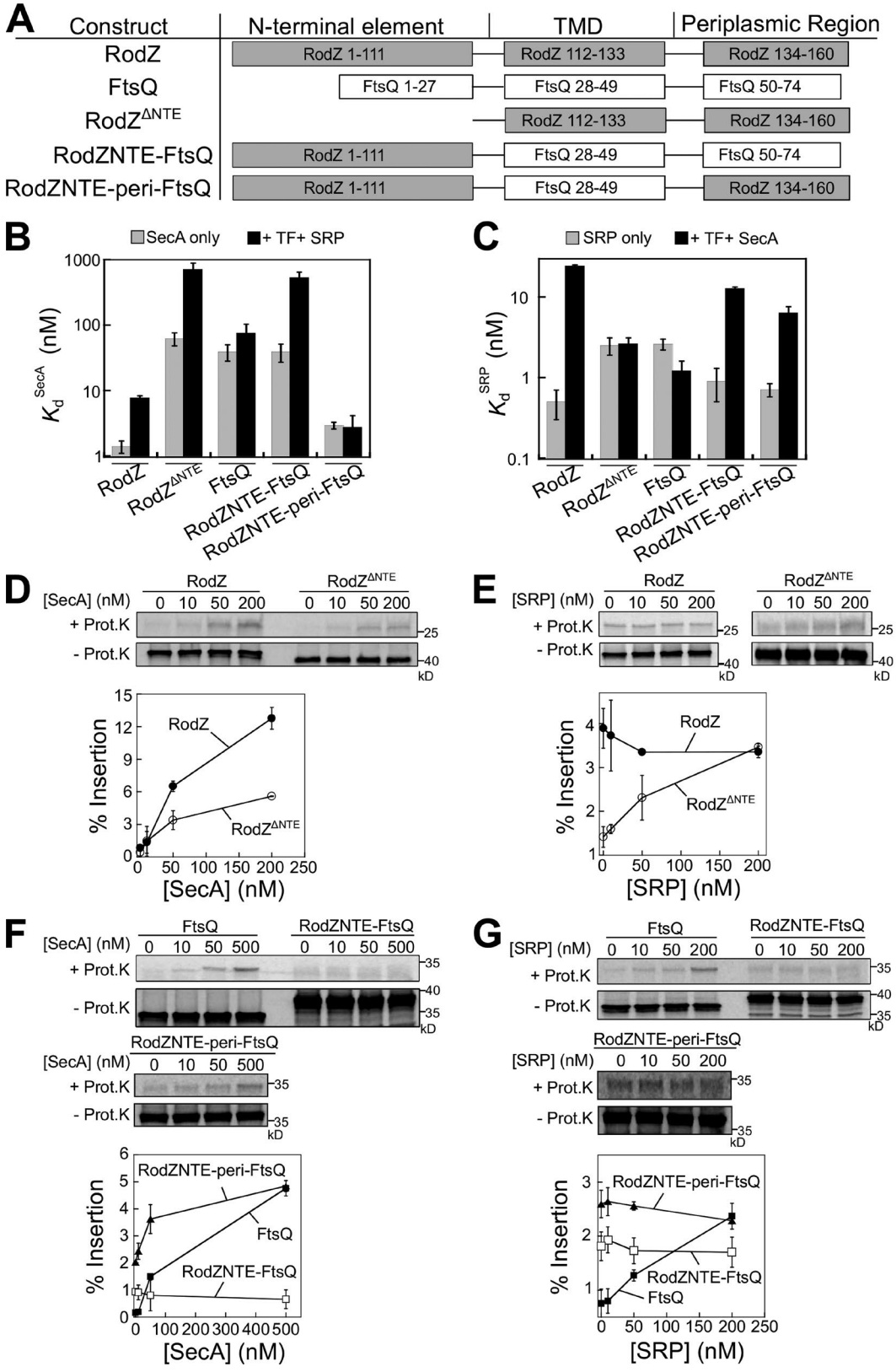

Figure 6. **The NTE and early periplasmic region of RodZ together dictate the selection of a membrane protein into the SecA versus SRP pathway.** (A) Scheme of the sequence elements of the substrate variants tested in this figure. Detailed sequences are in Table S1. (B and C) Summary of the K_d values of RNCs bearing different nascent chains for binding to SecA (B) or SRP (C) derived from the equilibrium titrations in Fig. S4. All titrations contained 20 nM RNCs and 2 µM TF, 400 nM SRP, or 2 µM SecA where indicated. (D and E) In vitro translocation assays of WT RodZ or mutant RodZ$^{\Delta NTE}$ and their dependence on SecA (D) or SRP (E). (F and G) In vitro translocation assays of WT FtsQ and mutants RodZNTE-FtsQ and RodZNTE-peri-FtsQ. The dependence of the reaction on SecA was shown in F, and the dependence on SRP was shown in G. The reactions in D and F contained 3.8 µM TF, 400 nM Ffh, 1 µM FtsY, and indicated concentrations of SecA. The reactions in E and G contained 50 nM SecA, 3.8 µM TF, the indicated concentrations of SRP, and a fivefold excess of FtsY over SRP. Values represent mean ± SD; n = 2–3.

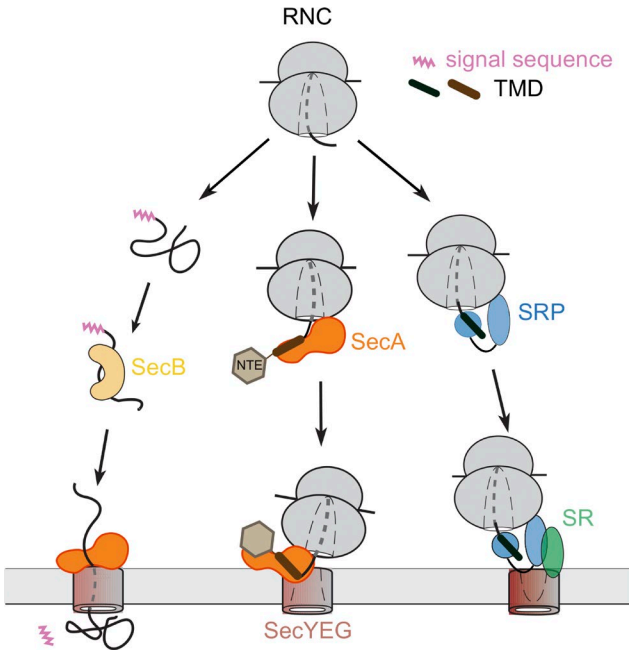

Figure 7. **Diverse targeting pathways deliver nascent proteins to the SecYEG translocon at the inner membrane.** Left path, proteins with weakly hydrophobic signal sequences are maintained soluble by SecB and targeted to membrane via interaction with SecA, which translocates the nascent polypeptide across SecYEG. Right path, proteins containing hydrophobic TMDs or signal sequences are cotranslationally recognized by SRP and targeted to SecYEG via the SRP/SR interaction. Middle path, proteins harboring internal TMDs are cotranslationally recognized and targeted by SecA.

Ariosa et al. [2015] for a formulation of the different models and their experimental predictions). However, as we have described extensively (Zhang et al., 2009, 2010), binding of SRP to an RNC does not necessarily turn on downstream steps in the targeting pathway, including efficient assembly of SRP with the SR, regulated GTP hydrolysis in the SRP/SR complex, and cargo unloading at the membrane translocon. Given the observation that RodZ does not require SRP for insertion in vitro and in vivo, the observed binding of SRP on RNC_{RodZ} likely represents a "standby" interaction mode of SRP that does not lead to SRP-dependent targeting.

The ribosome exit site is a crowded environment at which multiple protein biogenesis factors can bind and access the nascent polypeptide. The ability of SecA to cotranslationally interact with nascent proteins further increases the complexity of this environment. This raises intriguing questions as to how nascent proteins are selected by the proper biogenesis factor or factors, and the preference of both SecA and SRP for hydrophobic TMDs renders this selection particularly challenging. Although the precise mechanism remains to be determined, the results in this study provided important information. First, the extended NTE of RodZ effectively weakens the interaction of SRP with nascent proteins. This is analogous to the long NTEs preceding the signal sequences of bacterial autotransporters such as EspP, which also act as self-sufficient SRP avoidance sequences (Peterson et al., 2003; von Loeffelholz et al., 2013). Interestingly, the recently discovered SRP-independent pathway in yeast primarily targets ER-destined membrane proteins harboring internal TMDs (Ast et al., 2013; Aviram et al., 2016), suggesting that a long N-terminal sequence preceding a downstream TMD might be a general feature to disfavor engagement with the SRP machinery. In addition, the consecutive basic residues immediately upstream of the TMD facilitate SecA recruitment. Enrichment of N-terminal basic residues correlated with enhanced signal sequence binding and preprotein translocation by SecA (Akita et al., 1990; Hikita and Mizushima, 1992; Gelis et al., 2007). The same enrichment of basic residues was also observed in the NTE of EspP (Peterson et al., 2003) and might provide another distinguishing feature that favors the selection for SecA over SRP. Finally, the periplasmic region of RodZ after its TMD is also required for directing the substrate into the SecA-dependent targeting pathway. Acidic residues in the early periplasmic region have been shown to be important for the translocation of secretory protein across membrane (Kajava et al., 2000). The results in this study suggest a function of these acidic residues to directly interact with SecA to facilitate translocation. Given the challenges in recognizing degenerate topogenic signals on nascent proteins among a multitude of biogenesis factors, such a "multiplexed" recognition mechanism might be an effective strategy to ensure accurate nascent protein selection into the appropriate biogenesis pathway.

Materials and methods

Strains

The *E. coli* strains EO527 and WAM121 have been described previously (de Gier et al., 1996; Or et al., 2005). To construct the strain KC623 harboring mutant L23 (KC6 Δ*rplW*::kan $pL23_{F51A/E52A/E54A/E56A/E89A}$), DNA coding L23 mutations was cloned into pEK20 by Gibson assembly (Gibson et al., 2009) and transformed into the *E. coli* strain KC6 (A19 Δ*endA met*$^+$ Δ*tonA* Δ*speA* Δ*tnaA* Δ*sdaA* Δ*sdaB* Δ*gshA*; Calhoun and Swartz, 2006). The genomic L23 in KC6 harboring $pL23_{F51A/E52A/E54A/E56A/E89A}$ was then knocked out by λ-red recombination (Datsenko and Wanner, 2000).

Protein expression and purification

N-terminally His_6-tagged SecA (WT and mutant) was cloned in pET28a and expressed in BL21 (DE3) cells. Expression was induced by 0.5 mM IPTG at OD_{600} = 0.5 and 30°C for 4 h. Cells were lysed by FRENCH PRESS (Thermo Fisher Scientific) in SecA500 buffer (20 mM Hepes, pH 7.5, 500 mM KCl, 4 mM $MgCl_2$, and 4 mM β-mercaptoethanol [BME]) containing 10 mM imidazole and cOmplete protease inhibitor cocktail (Roche). Clarified lysate was loaded onto Ni-NTA resin and washed with SecA500 buffer. Protein was eluted with SecA500 buffer containing 250 mM imidazole. The His_6 tag was removed by tobacco etch virus protease digestion in SecA200 buffer (20 mM Hepes, pH 7.5, 200 mM KCl, 4 mM $MgCl_2$, 10 mM imidazole, and 4 mM BME) at 4°C overnight and reloaded onto Ni-NTA. Flowthrough was collected, exchanged into SecA50 buffer (20 mM Tris-HCl, pH 8.0, 50 mM KCl, 4 mM $MgCl_2$, and 2 mM DTT), and then further purified on MonoQ 10/100 GL (GE Healthcare) using a linear gradient of 50–1,000 mM KCl.

Ffh was expressed in pET3a vector with an *E. coli* BL21(DE3) pLysE strain (Peluso et al., 2000). At OD_{600} = 0.8, Ffh was induced by 1 mM IPTG at 37°C for 4 h. Cells were lysed in Ffh buffer 1 (20 mM Hepes, pH 8.0, 2 mM EDTA, 2 mM DTT, 250 mM NaCl, and 1 mM PMSF) by sonication. Clarified lysate was loaded onto an SP Sepharose fast flow column (GE Healthcare) equilibrated in Ffh buffer 1. Protein was eluted using a linear gradient of 250–1,000 mM NaCl. Ffh was further purified by a Superose 12 gel filtration column (GE Healthcare) in Ffh buffer 2 (20 mM Hepes, pH 8.0, 2 mM EDTA, 2 mM DTT, and 250 mM NaCl).

C-terminal His_6-tagged FtsY was cloned in pET9a vector and expressed in *E. coli* BL21(DE3) pLysS strain (Jagath et al., 2000). At OD_{600} = 0.6, FtsY was induced by 0.5 mM IPTG at 37°C for 5 h. Cells were lysed in FtsY buffer 1 (20 mM Hepes, pH 7.5, 2 mM EDTA, 150 mM NaCl, 0.01% [wt/vol] nikkol, 2 mM DTT, and 1 mM PMSF) by sonication. Lysate was clarified in Ti 45 rotor (Beckman Coulter) at 38,000 rpm for 45 min and loaded onto Q Sepharose Fast Flow column (GE Healthcare) equilibrated in FtsY buffer 1, and bound protein was eluted by a linear gradient of 150–500 mM NaCl. FtsY was further purified by a Superose 12 gel filtration column in FtsY buffer 2 (20 mM Hepes, pH 8.0, 2 mM EDTA, 2 mM DTT, and 250 mM NaCl). Pooled fractions were dialyzed against FtsY buffer 3 (20 mM Hepes, pH 7.5, and 150 mM KCl) and then loaded onto Ni-NTA equilibrated in buffer 3. Bound protein was washed with FtsY buffer 4 (20 mM Hepes, pH 7.5, 1 M KCl, and 10 mM imidazole) and eluted with FtsY buffer 4 (20 mM Hepes, pH 7.5, 150 mM KCl, and 200 mM imidazole). Protein was further dialyzed against FtsY buffer 5 (50 mM Tris-HCl, pH 7.4, 1 mM EDTA, and 2 mM DTT) and loaded onto MonoQ (10/100 GL) equilibrated in FtsY buffer 5. FtsY was eluted by a linear gradient of 150–1,000 mM NaCl.

TF was cloned in pH6 vector and expressed in *E. coli* DH5α strain transformed with pZA4 (Ariosa et al., 2015). Cells were grown at 30°C to OD_{600} = 0.6, induced by 0.5 mM IPTG for 3 h, and then lysed in TF buffer 1 (50 mM Tris-HCl, pH 7.5, 20 mM imidazole, 200 mM NaCl, 1 mM EDTA, 4 mM BME, and 1 mM PMSF) by FRENCH PRESS. Clarified lysate was loaded onto Ni-NTA equilibrated with TF buffer 1. TF was eluted with TF buffer 2 (50 mM Tris-HCl, pH 7.5, 500 mM imidazole, 200 mM NaCl, 1 mM BME, and 1 mM PMSF) and dialyzed against TF buffer 3 (50 mM Tris-HCl, pH 7.5, 50 mM NaCl, 1 mM EDTA, and 1 mM DTT). Protein was further purified on MonoQ 10/100 GL (GE Healthcare) using a linear gradient of 100–1,000 mM NaCl.

pHKSB366 encoding SecB was a gift from A. Karamyshev (Texas Tech University, Lubbock, TX; Fekkes et al., 1998). SecB was expressed in BL21(DE3) using 1 mM IPTG at OD_{600} = 1.0 at 37°C for 2 h. Cells were lysed by sonication in SecB buffer 1 (50 mM potassium phosphate, pH 7.5, and 300 mM NaCl) containing 20 mM imidazole. Clarified lysate was precipitated with 50% ammonium sulfate and centrifuged at 10,000 *g* for 10 min. The pellet was resuspended in SecB buffer 1 and loaded onto Ni-NTA preequilibrated with SecB buffer 1. SecB was eluted with SecB buffer 1 containing 500 mM imidazole followed by dialysis in 50 mM Tris, pH 7.5. After ultracentrifugation in TLA100.3 (Beckman Coulter) at 60,000 *g* for 1 h, the supernatant was loaded onto MonoQ equilibrated in SecB buffer 2 (50 mM Tris-HCl, pH 7.5, and 30 mM NaCl) and eluted with a linear gradient of 30–1,000 mM NaCl. The protein was desalted in SecB buffer 2.

SUMO and SUMO fusions to the periplasmic segments of RodZ or FtsQ were expressed using a pET28 vector encoding N-terminal His_6-tagged full-length SUMO family protein SMT3 from *Saccharomyces cerevisiae* fused to RodZ residues 134–160 or FtsQ residues 50–74 where applicable. Proteins were expressed in BL21(DE3) using 0.5 mM IPTG at OD_{600} = 0.5 and 37°C for 3 h. Cell was lysed by sonication in SUMO buffer 1 (20 mM Hepes, pH 7.5, 300 mM NaCl, and 4 mM BME) containing 20 mM imidazole and cOmplete protease inhibitor cocktail. Clarified lysate was loaded onto Ni-NTA resin and washed with SUMO buffer 1. Protein was eluted with SUMO buffer 1 containing 250 mM imidazole. Proteins were dialyzed against SUMO buffer 2 (20 mM Hepes, pH 7.5, 300 mM NaCl, 10% glycerol, and 2 mM TCEP) at 4°C and stored at −80°C.

RNC preparation

Cm-labeled RNCs were generated by IVT in S30 extract supplemented with Cm (Bachem), $tRNA^{Cm}$, and Cm tRNA synthetase as described previously (Schaffitzel et al., 2006). In brief, pUC19 plasmids (0.06 mg/ml) containing T7 promoter followed by nascent chain coding sequence and SecM arrest sequence (Table S1) were transcribed and translated in 5–10 ml reaction mixture containing 12 mM magnesium glutamate, 10 mM ammonium glutamate, 175 mM potassium glutamate, 1.2 mM ATP, 0.86 mM GTP, 0.86 mM CTP, 0.86 mM UTP, 34 µg/ml folinic acid, 0.17 mg/ml *E. coli* tRNA (Roche), amino acid mix (2 mM each), 33 mM phosphoenolpyrovate, 0.33 mM β-nicotinamide adenine dinucleotide, 0.26 mM CoA, 2.7 mM sodium oxalate, 1.5 mM spermidine, 1 mM putrescine, 4 µM anti–ssr1 oligonucleotide, 12 µM RF1 aptamer (Saraogi et al., 2011), 28% (vol/vol) S30 extract, 12 µM coumarine synthetase D286R (Wang et al., 2006), 2 µM T7 RNA polymerase, and 75 µM Cm (Bachem), pH 7.8, at 30°C for 1.5 h. Reaction samples were loaded onto a StrepTactin column (IBA) equilibrated in solution 1 (50 mM Hepes, pH 7.5, 100 mM KOAc, and 100 mM $Mg(OAc)_2$) and washed with solution 1 containing 500 mM KOAc. RNCs were eluted using solution 1 containing 1.5 mg/ml D-desthiobiotin (Sigma-Aldrich). $Strep_3$ tag was removed by thrombin (Roche). RNCs were sedimented in Ti 70 rotor (Beckman Coulter) at 42,000 rpm for 3.5 h and resuspended in SRP buffer (50 mM Hepes, pH 7.5, 150 mM KOAc, 10 mM $Mg(OAc)_2$, and 2 mM DTT) at 4°C overnight. To prepare RNCs harboring mutant L23(F51A/E52A/E54A/E56A/E89A), S30 extract was prepared from the strain KC623 harboring L23 mutant (KC6 Δ*rplW*::kan $pL23_{F51A/E52A/E54A/E56A/E89A}$; see the Strains section for strain construction).

RNaseA/EDTA treatment of RNCs

To release nascent chains from the ribosome, RNCs were incubated with 20 mM EDTA, pH 8.0, and 50 µg/ml RNaseA at 37°C for 30 min (Ziehr et al., 2010). To verify the effectiveness of this treatment, RNCs before and after the treatment were sedimented in a TLA100 (Beckman Coulter) rotor at 100,000 *g* for 2.5 h. The pellet was resuspended with SDS loading buffer at equal volume as the supernatant; both pellet and supernatant fractions were subject to SDS-PAGE analysis.

Fluorescent labeling

The single cysteine mutant Ffh (C406S/D421C) and the single cysteine mutant SecA(C98S/S12C) were purified as described in the Protein expression and purification section. They were reduced with 2 mM DTT at 4°C for 30 min followed by dialysis in labeling buffer (20 mM Hepes, pH 7.0, 300 mM KCl, 10% glycerol, and 2 mM TCEP) to remove DTT. 70 µM Ffh (C406S/D421C) was mixed with a 30-fold excess of BDP maleimide, and 40 µM SecA (C98S/S12C) was mixed with a 20-fold excess of BDP maleimide on a rotary shaker at 4°C for 4 h. After quenching with 10 mM DTT, free dye was removed by chromatography on Sephadex G-25 column (Sigma-Aldrich) in SRP buffer (50 mM Hepes, pH 7.5, 150 mM KOAc, 10 mM $Mg(OAc)_2$, 2 mM DTT, and 10% glycerol). Labeling efficiencies were 86% for Ffh and 99% for SecA, respectively, determined using the adsorption coefficient of $\varepsilon = 73{,}000\ M^{-1}cm^{-1}$ for BDP maleimide in aqueous buffer (Stray et al., 2006) and mass spectrometry. The cysteines in the zinc finger domain of SecA are coordinated by Zn^{2+} and were not labeled (not depicted).

Fluorescence measurements

All proteins were ultracentrifuged in TLA100 (Beckman Coulter) at 100,000 *g* for 1 h before fluorescence measurements. Fluorescence experiments were performed as described previously (Zhang et al., 2010; Ariosa et al., 2015) at room temperature in assay buffer (50 mM Hepes, pH 7.5, 150 mM KOAc, 10 mM $Mg(OAc)_2$, 2 mM DTT, and 0.1 mg/ml BSA). Experiments were performed on Fluorolog-3 (HORIBA) using 360-nm excitation wavelength (slit, 4 nm) and 455-nm emission wavelength (slit, 10 nm) for equilibrium titrations. Equilibrium titrations were performed using 20 nM Cm-labeled RNC, indicated

concentrations of cytosolic competitors where applicable, and SecA or Ffh as the titrant. The observed FRET value at individual titrant concentrations ($FRET_{obsd}$) were calculated from Eq. 1,

$$FRET_{obsd} = 1 - \frac{D_A}{D_0}, \quad (1)$$

in which D_0 is the donor fluorescence signal in the absence of the FRET accepter, and D_A is the donor fluorescence signal in the presence of the accepter-labeled titrant.

The concentration dependence of $FRET_{obsd}$ in a titration curve was fit to Eq. 2 (Cooper, 2004),

$$FRET_{obsd} = FRET_{max} \times \frac{\left[RNC\right] + \left[titrant\right] + K_d - \sqrt{\left(\left[RNC\right] + \left[titrant\right] + K_d\right)^2 - 4 \times \left[RNC\right] \times \left[titrant\right]}}{2 \times [RNC]} \quad (2)$$

in which [RNC], [titrant], and FRET are input values, $FRET_{max}$ is the FRET value at saturating titrant concentration, and K_d is the dissociation constant of the complex of interest.

To facilitate comparison of complexes with different K_d values, $FRET_{obsd}$ was further divided by the $FRET_{max}$ values obtained from fitting the data to Eq. 2 to generate normalized titration curves. These curves are described by Eq. 3:

$$\text{Normalized } \Delta F = 1 \times \frac{[RNC] + [titrant] + K_d - \sqrt{\left(\left[RNC\right] + \left[titrant\right] + K_d\right)^2 - 4 \times \left[RNC\right] \times \left[titrant\right]}}{2 \times [RNC]}. \quad (3)$$

To measure the binding of the SUMO-RodZPeri fusion protein to SecA, 50 nM $SecA^{BDP}$ was preincubated with 20 nM Cm-labeled RNC_{RodZ}. Increasing concentrations of SUMO-RodZ(peri) were added as a competitive inhibitor of the FRET between $SecA^{BDP}$ and RNC^{Cm}, and the observed changes in fluorescence intensity of Cm-labeled RNC_{RodZ} (F_{obsd}) were recorded. The data were fit to Eq. 8, derived by numerically solving the four relationships (Eqs. 4, 5, 6, and 7) according to the reaction scheme in Fig. 3 G:

$$\left[SecA^{BDP}\right] + \left[SecA^{BDP} \cdot RNC^{Cm}\right] + \left[SecA^{BDP} \cdot \text{SUMO variant}\right] = 50 \text{ nM}, \quad (4)$$

$$\left[SecA^{BDP} \cdot RNC^{Cm}\right] + \left[RNC^{Cm}\right] = 20 \text{ nM}, \quad (5)$$

$$\frac{[SecA^{BDP}] \times [RNC^{Cm}]}{[SecA^{BDP} \cdot RNC^{Cm}]} = K_d = 1 \text{ nM}, \quad (6)$$

$$\frac{[SecA^{BDP}] \times [SU]}{[SecA^{BDP} \cdot \text{SUMO variant}]} = K_i, \quad (7)$$

$$F_{obsd} = F_0 + m \times \frac{-[SU] - 31 \times K_i + \sqrt{[SU]^2 + 142 \times [SU] \times K_i + 1{,}041 \times K_i^2}}{2 \times K_i}. \quad (8)$$

In Eq 8, [SU] is the concentration of SUMO variant, K_i is the inhibition constant of the competitors for SecA, F_0 is the initial fluorescence intensity of Cm-labeled RNC_{RodZ} in the $SecA^{BDP}$–RNC^{Cm} complex, and m is the contribution to fluorescence intensity per nanomole of RNC^{Cm}.

In vivo translocation assay of NTS-TrxA fusions

pEK20 plasmids coding NTS-TrxA-myc fusion proteins were transformed into *E. coli* strains EO527 and WAM121, in which the expression of SecA and Ffh, respectively, were under control of the arabinose promoter (de Gier et al., 1996; Or et al., 2005). To deplete Ffh, WAM121 cells were grown to OD_{600} = 0.5 in LB supplemented with 0.02% (wt/vol) L-arabinose, washed twice with LB supplemented with 0.4% (wt/vol) D-glucose, and subcultured in LB supplemented with 0.4% (wt/vol) D-glucose. Ffh level was reduced to <5% after 3 h of media shift. SecA depletion in EO527 was performed similarly to Ffh depletion except that the subculture was grown for 5 h to deplete SecA. At OD_{600} = 0.4–0.6, NTS-TrxA-myc expression was induced by addition of IPTG (5 µM for RodZ and RodZNTE-FtsQ, 50 µM for all other constructs to achieve similar expression levels; Fig. S2 B) for 30 min at 37°C. Cells were harvested and resuspended in cold TrxA buffer 1 (0.1 M Tris-HCl, pH 8.0, and 20% sucrose). 0.5 mM EDTA, pH 8.0 and 50 µg/ml lysozyme were added, and the suspension was incubated at room temperature for 15 min. 20 mM $MgSO_4$ was added to stabilize spheroplasts. Spheroplasts were separated from the periplasmic fraction by centrifugation at 3,140 *g* for 10 min. For the proteinase K protection assay, spheroplasts were resuspended in cold TrxA buffer 2 (0.1 M Tris-HCl, pH 8.0, 20% sucrose, and 20 mM $MgSO_4$) and incubated with or without 0.5 mg/ml proteinase K on ice for 1 h. Reactions were stopped by addition of 5 mM PMSF. To further separate the cytosol from the membrane fraction, spheroplasts were resuspended in TrxA buffer 3 (50 mM Tris-HCl, pH 8.0, 150 mM NaCl, 1 mM EDTA, and 1 mM PMSF), lysed by one freeze-thaw cycle in liquid nitrogen, and clarified in TLA120.1 rotor at 63,000 rpm for 1 h. The supernatant was the cytosolic fraction, and the membrane pellet was resuspended with TrxA buffer 4 (20 mM Tris-HCl, pH 8.0, 5 mM EDTA, and 0.5% SDS). The translocation efficiencies for secretory proteins were calculated from the ratio of the secreted fraction to total protein amount. The translocation efficiencies for membrane proteins were calculated from the ratio of protein intensity after/before proteinase K digestion.

Western blot

Rabbit anti-SecA antibody was a gift from T.A. Rapoport (Harvard Medical School, Boston, MA). Rabbit anti-Ffh antibody was a gift from P. Walter (University of California, San Francisco, San Francisco, CA). Rabbit anti-YidC antibody was a gift from R.E. Dalbey (Ohio State University, Columbus, OH). The following antibodies were commercially available: rabbit anti-TrxA antibody (T0803; Sigma-Aldrich), mouse anti–β lactamase antibody (MA1-10712; Thermo Fisher Scientific), and rabbit anti–myc tag antibody (ab9106; Abcam). Primary antibodies were incubated with IRDye 800CW goat anti–rabbit IgG (925-32211; LI-COR Biosciences) or IRDye 800CW goat anti–mouse IgG (925-32210; LI-COR Biosciences) for detection. Protein band intensity was quantified by the Odyssey CLx imaging system (LI-COR Biosciences).

Preparation of U-IMVs

SecYEG was overexpressed in MRE600 by induction with 0.5 mM IPTG for 2 h. Cells were harvested in IMV buffer 1 (50 mM TEA-OAc, pH 7.5, 250 mM sucrose, 1 mM EDTA, 1 mM DTT, and 0.5 mM PMSF) and lysed at 8,000 psi by FRENCH PRESS. Unbroken cells were removed by centrifugation at 4,000 *g* for 10 min. Membranes were further pelleted in a Ti 70 rotor at 45,000 rpm for 2 h and resuspended in IMV buffer 1. The membrane suspension was layered onto a five-step sucrose gradient (0.8, 1.0, 1.2, 1.4, and 1.6 M sucrose in IMV buffer 1) and ultracentrifuged in SW32 (Beckman Coulter) at 24,000 rpm for 16 h. IMV fractions were collected from the lower one third

of the gradient as described previously (Müller and Blobel, 1984a). To make U-IMVs, four volumes of IMV buffer 2 (50 mM TEA-OAc, pH 7.5, 250 mM sucrose, 1 M KOAc, and 7.5 M urea) were added to IMVs. The mixture was incubated on ice for 1 h, after which the urea concentration was adjusted to 3 M before pelleting through a sucrose cushion (50 mM TEA-OAc, pH 7.5, 750 mM sucrose, 1 M KOAc, and 1 mM DTT) in TLA100.3 at 60,000 rpm for 2 h. The pellet was resuspended in IMV buffer 3 (50 mM TEA-OAc, pH 7.5, 250 mM sucrose, and 1 mM DTT; Müller and Blobel, 1984b; Helde et al., 1997).

In vitro translocation assay in PURE system

Translation was performed at 30°C using a PURExpress in vitro protein synthesis kit (New England Biolabs, Inc.) supplemented with [^{35}S] methionine (1.5 mCi/ml; PerkinElmer) and indicated concentrations of cytosolic factors (SecA, SecB, Ffh, FtsY, or TF). Unless otherwise indicated, 0.5 mg/ml U-IMVs was added 5 min after initiation of translation. The reaction was continued for 85 min at 30°C, after which it was split equally into two samples, one of which was digested with 0.5 mg/ml proteinase K for 30 min at 25°C. Digestion was stopped by addition of 5 mM PMSF, after which the sample was incubated on ice for 10 min. Samples with and without proteinase K treatment were analyzed by SDS-PAGE and autoradiography. The insertion efficiency was calculated from the ratio of the intensity of substrate protein bands after and before proteinase K treatment. The loss of methionine or methionines after proteinase K digestion was corrected before calculation of insertion efficiency.

ProOmpA translocation in wheat germ lysate

ProOmpA mRNA was in vitro transcribed and purified as described previously (Behrmann et al., 1998). ProOmpA was translated using wheat germ extract (Promega) in the presence of [^{35}S]methionine (1.5 mCi/ml) at 26°C for 30 min, followed by incubation with U-IMVs at 37°C for 15 min in the presence of 10 mM phosphocreatine, 0.05 mg/ml creatine kinase, 4 mM $Mg(OAc)_2$, 2 mM ATP, 0.5 mg/ml BSA, 10 mM DTT, and the indicated concentrations of SecA. Samples were digested with 0.1 mg/ml proteinase K on ice for 15 min. Digestion was stopped by addition of 5 mM PMSF. All samples were precipitated by TCA and analyzed by SDS-PAGE and autoradiography.

Online supplemental material

Fig. S1 shows the controls for titration experiments and raw FRET titrations before normalization. Fig. S2 shows the SRP and SecA dependence of the targeting and translocation of TrxA fusion constructs in vivo. Fig. S3 shows replicates for the SecA/SRP dependence of translocation reactions across U-IMVs in vitro. Fig. S4 shows the equilibrium titration curves to measure the binding of SecA and SRP to RNCs bearing the nascent chains of RodZ, RodZ$^{\Delta NTE}$, FtsQ, RodZNTE-FtsQ, and RodZNTE-peri-FtsQ. Table S1 summarizes the sequence of various substrates used in RNC binding and in vivo translocation assays.

Acknowledgments

We thank Stephen H. White and Eric Lindner for discussions and members of the Shan group for comments on the manuscript.

This work was supported by National Institutes of Health grant GM107368A and the Gordon and Betty Moore Foundation through grant GBMF2939 to S.-o. Shan.

The authors declare no competing financial interests.

Author contributions: S. Wang designed and performed most of the experiments. C.-l Yang assisted in measuring the binding affinity of RNCs to SecA and SRP. S. Wang and S.-o. Shan wrote the paper. S.-o. Shan conceived the project. All authors reviewed the manuscript.

Submitted: 5 April 2017
Revised: 17 July 2017
Accepted: 2 August 2017

References

Akita, M., S. Sasaki, S. Matsuyama, and S. Mizushima. 1990. SecA interacts with secretory proteins by recognizing the positive charge at the amino terminus of the signal peptide in *Escherichia coli*. *J. Biol. Chem.* 265:8164–8169.

Ariosa, A., J.H. Lee, S. Wang, I. Saraogi, and S.O. Shan. 2015. Regulation by a chaperone improves substrate selectivity during cotranslational protein targeting. *Proc. Natl. Acad. Sci. USA.* 112:E3169–E3178. http://dx.doi.org/10.1073/pnas.1422594112

Ast, T., G. Cohen, and M. Schuldiner. 2013. A network of cytosolic factors targets SRP-independent proteins to the endoplasmic reticulum. *Cell.* 152:1134–1145. http://dx.doi.org/10.1016/j.cell.2013.02.003

Aviram, N., T. Ast, E.A. Costa, E.C. Arakel, S.G. Chuartzman, C.H. Jan, S. Haßdenteufel, J. Dudek, M. Jung, S. Schorr, et al. 2016. The SND proteins constitute an alternative targeting route to the endoplasmic reticulum. *Nature.* 540:134–138. http://dx.doi.org/10.1038/nature20169

Bauer, B.W., T. Shemesh, Y. Chen, and T.A. Rapoport. 2014. A "push and slide" mechanism allows sequence-insensitive translocation of secretory proteins by the SecA ATPase. *Cell.* 157:1416–1429. http://dx.doi.org/10.1016/j.cell.2014.03.063

Behrmann, M., H.G. Koch, T. Hengelage, B. Wieseler, H.K. Hoffschulte, and M. Müller. 1998. Requirements for the translocation of elongation-arrested, ribosome-associated OmpA across the plasma membrane of *Escherichia coli*. *J. Biol. Chem.* 273:13898–13904. http://dx.doi.org/10.1074/jbc.273.22.13898

Calhoun, K.A., and J.R. Swartz. 2006. Total amino acid stabilization during cell-free protein synthesis reactions. *J. Biotechnol.* 123:193–203. http://dx.doi.org/10.1016/j.jbiotec.2005.11.011

Chatzi, K.E., M.F. Sardis, A. Tsirigotaki, M. Koukaki, N. Šoštarić, A. Konijnenberg, F. Sobott, C.G. Kalodimos, S. Karamanou, and A. Economou. 2017. Preprotein mature domains contain translocase targeting signals that are essential for secretion. *J. Cell Biol.* 216:1357–1369. http://dx.doi.org/10.1083/jcb.201609022

Cooper, A. 2004. Biophysical Chemistry. Royal Society of Chemistry, Cambridge, England, UK.

Datsenko, K.A., and B.L. Wanner. 2000. One-step inactivation of chromosomal genes in *Escherichia coli* K-12 using PCR products. *Proc. Natl. Acad. Sci. USA.* 97:6640–6645. http://dx.doi.org/10.1073/pnas.120163297

de Gier, J.W., P. Mansournia, Q.A. Valent, G.J. Phillips, J. Luirink, and G. von Heijne. 1996. Assembly of a cytoplasmic membrane protein in *Escherichia coli* is dependent on the signal recognition particle. *FEBS Lett.* 399:307–309. http://dx.doi.org/10.1016/S0014-5793(96)01354-3

Estrozi, L.F., D. Boehringer, S.O. Shan, N. Ban, and C. Schaffitzel. 2011. Cryo-EM structure of the *E. coli* translating ribosome in complex with SRP and its receptor. *Nat. Struct. Mol. Biol.* 18:88–90. http://dx.doi.org/10.1038/nsmb.1952

Fekkes, P., J.G. de Wit, J.P. van der Wolk, H.H. Kimsey, C.A. Kumamoto, and A.J. Driessen. 1998. Preprotein transfer to the *Escherichia coli* translocase requires the co-operative binding of SecB and the signal sequence to SecA. *Mol. Microbiol.* 29:1179–1190. http://dx.doi.org/10.1046/j.1365-2958.1998.00997.x

Gamerdinger, M., M.A. Hanebuth, T. Frickey, and E. Deuerling. 2015. The principle of antagonism ensures protein targeting specificity at the endoplasmic reticulum. *Science.* 348:201–207 http://dx.doi.org/. http://dx.doi.org/10.1126/science.aaa5335

Gebert, J.F., B. Overhoff, M.D. Manson, and W. Boos. 1988. The Tsr chemosensory transducer of *Escherichia coli* assembles into the cytoplasmic membrane via a *SecA*-dependent process. *J. Biol. Chem.* 263:16652–16660.

Gelis, I., A.M. Bonvin, D. Keramisanou, M. Koukaki, G. Gouridis, S. Karamanou, A. Economou, and C.G. Kalodimos. 2007. Structural basis for signal-sequence recognition by the translocase motor SecA as determined by NMR. *Cell.* 131:756–769. http://dx.doi.org/10.1016/j.cell.2007.09.039

Gibson, D.G., L. Young, R.Y. Chuang, J.C. Venter, C.A. Hutchison III, and H.O. Smith. 2009. Enzymatic assembly of DNA molecules up to several hundred kilobases. *Nat. Methods.* 6:343–345. http://dx.doi.org/10.1038/nmeth.1318

Gouridis, G., S. Karamanou, I. Gelis, C.G. Kalodimos, and A. Economou. 2009. Signal peptides are allosteric activators of the protein translocase. *Nature.* 462:363–367. http://dx.doi.org/10.1038/nature08559

Hartl, F.U., S. Lecker, E. Schiebel, J.P. Hendrick, and W. Wickner. 1990. The binding cascade of SecB to SecA to SecY/E mediates preprotein targeting

to the E. coli plasma membrane. *Cell.* 63:269–279. http://dx.doi.org/10.1016/0092-8674(90)90160-G

Helde, R., B. Wiesler, E. Wachter, A. Neubüser, H.K. Hoffschulte, T. Hengelage, K.L. Schimz, R.A. Stuart, and M. Müller. 1997. Comparative characterization of SecA from the alpha-subclass purple bacterium Rhodobacter capsulatus and Escherichia coli reveals differences in membrane and precursor specificity. *J. Bacteriol.* 179:4003–4012. http://dx.doi.org/10.1128/jb.179.12.4003-4012.1997

Hikita, C., and S. Mizushima. 1992. The requirement of a positive charge at the amino terminus can be compensated for by a longer central hydrophobic stretch in the functioning of signal peptides. *J. Biol. Chem.* 267:12375–12379.

Hoffschulte, H.K., B. Drees, and M. Müller. 1994. Identification of a soluble SecA/SecB complex by means of a subfractionated cell-free export system. *J. Biol. Chem.* 269:12833–12839.

Huber, D., D. Boyd, Y. Xia, M.H. Olma, M. Gerstein, and J. Beckwith. 2005a. Use of thioredoxin as a reporter to identify a subset of *Escherichia coli* signal sequences that promote signal recognition particle-dependent translocation. *J. Bacteriol.* 187:2983–2991. http://dx.doi.org/10.1128/JB.187.9.2983-2991.2005

Huber, D., M.I. Cha, L. Debarbieux, A.G. Planson, N. Cruz, G. López, M.L. Tasayco, A. Chaffotte, and J. Beckwith. 2005b. A selection for mutants that interfere with folding of *Escherichia coli* thioredoxin-1 in vivo. *Proc. Natl. Acad. Sci. USA.* 102:18872–18877. http://dx.doi.org/10.1073/pnas.0509583102

Huber, D., N. Rajagopalan, S. Preissler, M.A. Rocco, F. Merz, G. Kramer, and B. Bukau. 2011. SecA interacts with ribosomes in order to facilitate posttranslational translocation in bacteria. *Mol. Cell.* 41:343–353. http://dx.doi.org/10.1016/j.molcel.2010.12.028

Huber, D., M. Jamshad, R. Hanmer, D. Schibich, K. Döring, I. Marcomini, G. Kramer, and B. Bukau. 2016. SecA cotranslationally interacts with nascent substrate proteins in vivo. *J. Bacteriol.* 199:e00622-16.

Jagath, J.R., M.V. Rodnina, and W. Wintermeyer. 2000. Conformational changes in the bacterial SRP receptor FtsY upon binding of guanine nucleotides and SRP. *J. Mol. Biol.* 295:745–753. http://dx.doi.org/10.1006/jmbi.1999.3427

Kajava, A.V., S.N. Zolov, A.E. Kalinin, and M.A. Nesmeyanova. 2000. The net charge of the first 18 residues of the mature sequence affects protein translocation across the cytoplasmic membrane of gram-negative bacteria. *J. Bacteriol.* 182:2163–2169. http://dx.doi.org/10.1128/JB.182.8.2163-2169.2000

Karamyshev, A.L., and A.E. Johnson. 2005. Selective SecA association with signal sequences in ribosome-bound nascent chains: A potential role for SecA in ribosome targeting to the bacterial membrane. *J. Biol. Chem.* 280:37930–37940. http://dx.doi.org/10.1074/jbc.M509100200

Kihara, A., and K. Ito. 1998. Translocation, folding, and stability of the HflKC complex with signal anchor topogenic sequences. *J. Biol. Chem.* 273:29770–29775. http://dx.doi.org/10.1074/jbc.273.45.29770

Kuruma, Y., K. Nishiyama, Y. Shimizu, M. Müller, and T. Ueda. 2005. Development of a minimal cell-free translation system for the synthesis of presecretory and integral membrane proteins. *Biotechnol. Prog.* 21:1243–1251. http://dx.doi.org/10.1021/bp049553u

Lindner, E., and S.H. White. 2014. Topology, dimerization, and stability of the single-span membrane protein CadC. *J. Mol. Biol.* 426:2942–2957. http://dx.doi.org/10.1016/j.jmb.2014.06.006

Luirink, J., and I. Sinning. 2004. SRP-mediated protein targeting: structure and function revisited. *Biochim. Biophys. Acta.* 1694:17–35.

Müller, M., and G. Blobel. 1984a. In vitro translocation of bacterial proteins across the plasma membrane of Escherichia coli. *Proc. Natl. Acad. Sci. USA.* 81:7421–7425. http://dx.doi.org/10.1073/pnas.81.23.7421

Müller, M., and G. Blobel. 1984b. Protein export in Escherichia coli requires a soluble activity. *Proc. Natl. Acad. Sci. USA.* 81:7737–7741. http://dx.doi.org/10.1073/pnas.81.24.7737

Nakatogawa, H., and K. Ito. 2002. The ribosomal exit tunnel functions as a discriminating gate. *Cell.* 108:629–636. http://dx.doi.org/10.1016/S0092-8674(02)00649-9

Neumann-Haefelin, C., U. Schäfer, M. Müller, and H.G. Koch. 2000. SRP-dependent co-translational targeting and SecA-dependent translocation analyzed as individual steps in the export of a bacterial protein. *EMBO J.* 19:6419–6426. http://dx.doi.org/10.1093/emboj/19.23.6419

Or, E., D. Boyd, S. Gon, J. Beckwith, and T. Rapoport. 2005. The bacterial ATPase SecA functions as a monomer in protein translocation. *J. Biol. Chem.* 280:9097–9105. http://dx.doi.org/10.1074/jbc.M413947200

Peluso, P., D. Herschlag, S. Nock, D.M. Freymann, A.E. Johnson, and P. Walter. 2000. Role of 4.5S RNA in assembly of the bacterial signal recognition particle with its receptor. *Science.* 288:1640–1643. http://dx.doi.org/10.1126/science.288.5471.1640

Peterson, J.H., C.A. Woolhead, and H.D. Bernstein. 2003. Basic amino acids in a distinct subset of signal peptides promote interaction with the signal recognition particle. *J. Biol. Chem.* 278:46155–46162. http://dx.doi.org/10.1074/jbc.M309082200

Qi, H.Y., and H.D. Bernstein. 1999. SecA is required for the insertion of inner membrane proteins targeted by the *Escherichia coli* signal recognition particle. *J. Biol. Chem.* 274:8993–8997. http://dx.doi.org/10.1074/jbc.274.13.8993

Randall, L.L. 1983. Translocation of domains of nascent periplasmic proteins across the cytoplasmic membrane is independent of elongation. *Cell.* 33:231–240. http://dx.doi.org/10.1016/0092-8674(83)90352-5

Rawat, S., L. Zhu, E. Lindner, R.E. Dalbey, and S.H. White. 2015. SecA drives transmembrane insertion of RodZ, an unusual single-span membrane protein. *J. Mol. Biol.* 427:1023–1037. http://dx.doi.org/10.1016/j.jmb.2014.05.005

Sääf, A., H. Andersson, G. Gafvelin, and G. von Heijne. 1995. SecA-dependence of the translocation of a large periplasmic loop in the *Escherichia coli* MalF inner membrane protein is a function of sequence context. *Mol. Membr. Biol.* 12:209–215. http://dx.doi.org/10.3109/09687689509027509

Samuelson, J.C., M. Chen, F. Jiang, I. Möller, M. Wiedmann, A. Kuhn, G.J. Phillips, and R.E. Dalbey. 2000. YidC mediates membrane protein insertion in bacteria. *Nature.* 406:637–641. http://dx.doi.org/10.1038/35020586

Saraogi, I., D. Zhang, S. Chandrasekaran, and S.O. Shan. 2011. Site-specific fluorescent labeling of nascent proteins on the translating ribosome. *J. Am. Chem. Soc.* 133:14936–14939. http://dx.doi.org/10.1021/ja206626g

Schaffitzel, C., M. Oswald, I. Berger, T. Ishikawa, J.P. Abrahams, H.K. Koerten, R.I. Koning, and N. Ban. 2006. Structure of the *E. coli* signal recognition particle bound to a translating ribosome. *Nature.* 444:503–506. http://dx.doi.org/10.1038/nature05182

Schibich, D., F. Gloge, I. Pöhner, P. Björkholm, R.C. Wade, G. von Heijne, B. Bukau, and G. Kramer. 2016. Global profiling of SRP interaction with nascent polypeptides. *Nature.* 536:219–223. http://dx.doi.org/10.1038/nature19070

Schierle, C.F., M. Berkmen, D. Huber, C. Kumamoto, D. Boyd, and J. Beckwith. 2003. The DsbA signal sequence directs efficient, cotranslational export of passenger proteins to the *Escherichia coli* periplasm via the signal recognition particle pathway. *J. Bacteriol.* 185:5706–5713. http://dx.doi.org/10.1128/JB.185.19.5706-5713.2003

Scotti, P., Q. Valent, E. Manting, M. Urbanus, A. Driessen, B. Oudega, and J. Luirink. 1999. SecA is not required for signal recognition particle-mediated targeting and initial membrane insertion of a nascent inner membrane protein. *J. Biol. Chem.* 274:29883–29888. http://dx.doi.org/10.1074/jbc.274.42.29883

Shimizu, Y., A. Inoue, Y. Tomari, T. Suzuki, T. Yokogawa, K. Nishikawa, and T. Ueda. 2001. Cell-free translation reconstituted with purified components. *Nat. Biotechnol.* 19:751–755. http://dx.doi.org/10.1038/90802

Siegel, V., and P. Walter. 1988. The affinity of signal recognition particle for presecretory proteins is dependent on nascent chain length. *EMBO J.* 7:1769–1775.

Singh, R., C. Kraft, R. Jaiswal, K. Sejwal, V.B. Kasaragod, J. Kuper, J. Bürger, T. Mielke, J. Luirink, and S. Bhushan. 2014. Cryo-electron microscopic structure of SecA protein bound to the 70S ribosome. *J. Biol. Chem.* 289:7190–7199. http://dx.doi.org/10.1074/jbc.M113.506634

Stray, S.J., J.M. Johnson, B.G. Kopek, and A. Zlotnick. 2006. An in vitro fluorescence screen to identify antivirals that disrupt hepatitis B virus capsid assembly. *Nat. Biotechnol.* 24:358–362. http://dx.doi.org/10.1038/nbt1187

Traxler, B., and C. Murphy. 1996. Insertion of the polytopic membrane protein MalF is dependent on the bacterial secretion machinery. *J. Biol. Chem.* 271:12394–12400. http://dx.doi.org/10.1074/jbc.271.21.12394

Ulbrandt, N.D., J.A. Newitt, and H.D. Bernstein. 1997. The E. coli signal recognition particle is required for the insertion of a subset of inner membrane proteins. *Cell.* 88:187–196. http://dx.doi.org/10.1016/S0092-8674(00)81839-5

van der Laan, M., P. Bechtluft, S. Kol, N. Nouwen, and A.J. Driessen. 2004. F1F0 ATP synthase subunit c is a substrate of the novel YidC pathway for membrane protein biogenesis. *J. Cell Biol.* 165:213–222. http://dx.doi.org/10.1083/jcb.200402100

von Loeffelholz, O., K. Knoops, A. Ariosa, X. Zhang, M. Karuppasamy, K. Huard, G. Schoehn, I. Berger, S.O. Shan, and C. Schaffitzel. 2013. Structural basis of signal sequence surveillance and selection by the SRP–FtsY complex. *Nat. Struct. Mol. Biol.* 20:604–610. http://dx.doi.org/10.1038/nsmb.2546

Walter, P., I. Ibrahimi, and G. Blobel. 1981. Translocation of proteins across the endoplasmic reticulum. I. Signal recognition protein (SRP) binds to in-

vitro-assembled polysomes synthesizing secretory protein. *J. Cell Biol.* 91:545–550. http://dx.doi.org/10.1083/jcb.91.2.545

Wang, J., J. Xie, and P.G. Schultz. 2006. A genetically encoded fluorescent amino acid. *J. Am. Chem. Soc.* 128:8738–8739. http://dx.doi.org/10.1021/ja062666k

Weiss, J.B., P.H. Ray, and P.J. Bassford Jr. 1988. Purified secB protein of Escherichia coli retards folding and promotes membrane translocation of the maltose-binding protein in vitro. *Proc. Natl. Acad. Sci. USA.* 85:8978–8982. http://dx.doi.org/10.1073/pnas.85.23.8978

Wickström, D., S. Wagner, L. Baars, A.J. Ytterberg, M. Klepsch, K.J. van Wijk, J. Luirink, and J.W. de Gier. 2011. Consequences of depletion of the signal recognition particle in *Escherichia coli*. *J. Biol. Chem.* 286:4598–4609. http://dx.doi.org/10.1074/jbc.M109.081935

Wolfe, P.B., M. Rice, and W. Wickner. 1985. Effects of two *sec* genes on protein assembly into the plasma membrane of *Escherichia coli*. *J. Biol. Chem.* 260:1836–1841.

Zhang, X., and S.O. Shan. 2014. Fidelity of cotranslational protein targeting by the signal recognition particle. *Annu. Rev. Biophys.* 43:381–408. http://dx.doi.org/10.1146/annurev-biophys-051013-022653

Zhang, D., M. Sweredoski, R. Graham, S. Hess, and S. Shan. 2012. Novel proteomic tools reveal essential roles of SRP and importance of proper membrane protein biogenesis. *Mol. Cell. Proteomics.* 11. http://dx.doi.org/10.1074/mcp.M111.011585

Zhang, J., X. Pan, K. Yan, S. Sun, N. Gao, and S.F. Sui. 2015. Mechanisms of ribosome stalling by SecM at multiple elongation steps. *eLife.* 4:e09684. http://dx.doi.org/10.7554/eLife.09684

Zhang, X., C. Schaffitzel, N. Ban, and S. Shan. 2009. Multiple conformational switches in a GTPase complex control co-translational protein targeting. *Proc. Natl. Acad. Sci. USA.* 106:1754–1759.

Zhang, X., R. Rashid, K. Wang, and S.O. Shan. 2010. Sequential checkpoints govern substrate selection during cotranslational protein targeting. *Science.* 328:757–760. http://dx.doi.org/10.1126/science.1186743

Ziehr, D.R., J.P. Ellis, P.H. Culviner, and S. Cavagnero. 2010. Production of ribosome-released nascent proteins with optimal physical properties. *Anal. Chem.* 82:4637–4643. http://dx.doi.org/10.1021/ac902952b

Zoschke, R., and A. Barkan. 2015. Genome-wide analysis of thylakoid-bound ribosomes in maize reveals principles of cotranslational targeting to the thylakoid membrane. *Proc. Natl. Acad. Sci. USA.* 112:E1678–E1687. http://dx.doi.org/10.1073/pnas.1424655112